First publ. in: European Journal of Biochemistry 268 (2001), 21, pp. 5504-5520

# pH and kinetic isotope effects in D-amino acid oxidase catalysis

## Evidence for a concerted mechanism in substrate dehydrogenation via hydride transfer

**Christopher M. Harris[1,*], Loredano Pollegioni[1] and Sandro Ghisla[2]**

[1]*Department of Structural and Functional Biology, University of Insubria, Varese, Italy;* [2]*Faculty of Biology, University of Konstanz, Germany*

The effects of pH, solvent isotope, and primary isotope replacement on substrate dehydrogenation by *Rhodotorula gracilis* D-amino acid oxidase were investigated. The rate constant for enzyme-FAD reduction by D-alanine increases ≈ fourfold with pH, reflecting apparent p$K_a$ values of ≈ 6 and ≈ 8, and reaches plateaus at high and low pH. Such profiles are observed in all presteady-state and steady-state kinetic experiments, using both D-alanine and D-asparagine as substrates, and are inconsistent with the operation of a base essential to catalysis. A solvent deuterium isotope effect of 3.1 ± 1.1 is observed on the reaction with D-alanine at pH 6; it decreases to 1.2 ± 0.2 at pH 10. The primary substrate isotope effect on the reduction rate with [2-D]D-alanine is 9.1 ± 1.5 at low and 2.3 ± 0.3 at high pH. At pH 6.0, the solvent isotope effect is 2.9 ± 0.8 with [2-D]D-alanine, and the primary isotope effect is 8.4 ± 2.4 in $D_2O$. Thus, primary and solvent kinetic isotope effects (KIEs) are independent of the presence of the other isotope, i.e. the 'double' kinetic isotope effect is the product of the individual KIEs, consistent with a transition state in which rupture of the two bonds of the substrate to hydrogen is concerted. These results support a hydride transfer mechanism for the dehydrogenation reaction in D-amino acid oxidase and argue against the occurrence of any intermediates in the process. A p$K_{a,app}$ of ≈ 8 is interpreted to arise from the microscopic ionization of the substrate amino acid α-amino group, but also includes contributions from kinetic parameters.

*Keywords*: flavoproteins; reaction mechanism; isotope effects; hydride transfer; pH effects.

D-Amino acid oxidase (EC 1.4.3.3, DAAO) catalyzes the two-electron dehydrogenation of D-amino acids to the corresponding imino acids (subsequently hydrolyzed to the α-keto acids and ammonia) with the concomitant reduction of the enzyme-bound FAD to $FAD_{red}H^-$. Oxidized enzyme flavin is regenerated by reduction of molecular oxygen to hydrogen peroxide [1].

DAAO was first isolated from pig kidney (pkDAAO), and it was the first enzyme shown to utilize FAD as a cofactor [2]. The physiological role of pkDAAO remains unclear [1], but possible functions include the catabolism of bacterial cell wall components and the breakdown of the proposed neurotransmitter D-serine [3]. D-Amino acid oxidase from the yeast *Rhodotorula gracilis* (RgDAAO) possesses several properties that make it more convenient for mechanistic studies than pkDAAO. Both enzymes exist as homodimers, but only pkDAAO dissociates into monomers with ensuing changes in kinetic properties [1]. Binding of FAD is much tighter with RgDAAO [4]. In addition, RgDAAO is more resistant to extreme conditions, such as exposure to heat and solvents [5]. The enzymes share 27% amino-acid identity [6].

The chemical mechanism of substrate dehydrogenation is still disputed within the class of flavin-containing amino-acid oxidases and α-hydroxy acid oxidases. The carbanion mechanism has been proposed for pkDAAO based mainly upon the observation that pkDAAO catalyzes the elimination of β-chloroalanine to pyruvate [7]. In this mechanism, an enzyme base is required to remove the substrate αC-H as a proton to form the carbanion intermediate. Subsequent transfer of electrons from the carbanion to the flavin N5 position would result in formation of $FAD_{red}H^-$ and imino acid. A p$K_a$ ≈ 21 was estimated for the αC-H of an amino acid [8]. There are two basic requirements for the carbanion mechanism to be operative: a base with an appropriate p$K_a$ and machinery that lowers the p$K_a$ of the amino-acid αC-H to levels compatible with catalysis. Indeed, optimal conditions for catalysis are realized when the two p$K_a$ values in question are of similar magnitude [9]. These basic requirements were recently shown to be met in the flavoenzyme acyl-CoA dehydrogenase where a combination proton abstraction/hydride transfer mechanism is operative [10]. Consequently, the p$K_a$ of the abstracted C-H is lowered from 21 to ≈ 8, and the p$K_a$ of the abstracting base, a glutamate, is increased from ≈ 3.5 to ≈ 8 [11].

An alternative to the carbanion mechanism is the transfer of hydride from the substrate to the flavin N5 position [12,13]. The results of a linear free energy correlation

*Correspondence to* S. Ghisla, Fachbereich Biologie, University of Konstanz, Postfach 5560 M644, D-78457 Konstanz, Germany. Fax/Tel.: + 49 7531 882291, E-mail: Sandro.Ghisla@uni-konstanz.de

*Abbreviations*: RgDAAO, *Rhodotorula gracilis* D-amino acid oxidase; pAAO, pig kidney D-amino acid oxidase; TvDAAO, *Trigonopsis variabilis* D-amino acid oxidase; LAAO, L-amino acid oxidase; KIE, kinetic isotope effect; $E_{ox}$, oxidized enzyme; $E_{red}$, reduced enzyme; $FADredH^-$, reduced anionic flavin; pL (H or D), reading of the pH electrode in $H_2O$ or $D_2O$.

*Enzymes*: D-amino acid oxidase (EC 1.4.3.3).

**Present address*: Department of Chemistry, University of Utah, Salt Lake City, UT, USA.

carried out with *Trigonopsis variabilis* DAAO (TvDAAO) and para-substituted phenylglycines clearly show that little or no charge develops in the transition state [14], inconsistent with a carbanion mechanism. Similarly, the finding that dehydrogenation of phenylglycine proceeds via concerted rupture of the two involved bonds to hydrogen is inconsistent with a carbanion intermediate [14]. The modes of binding of D-alanine and trifluoro-D-alanine at the active center of RgDAAO are clearly in favor of a hydride transfer mechanism [15]. A previously unexplained observation is the nature of the pH dependence of the dehydrogenation step in pkDAAO catalysis reported by Denu & Fitzpatrick [16]. These studies indicate the presence of an ionizing residue that must be deprotonated for activity, and were interpreted as suggesting base catalysis. Therefore, one aim of the present work was the characterization and identification of this ionization and the clarification of its mechanistic role by measuring the pH dependence of kinetic parameters. The three-dimensional structures [13,15,17] and site-directed mutagenesis [18–20] of pkDAAO and of RgDAAO concur in highlighting the absence of any active-site functional groups that may play essential roles in chemical catalysis. The second aim of the present work was to study how concerted the rupture of the substrate αC-H and αN-H bonds are in order to assess the occurrence of intermediates, using solvent and primary substrate kinetic isotope effects (KIEs), both individually and in combination. Studies were conducted primarily with D-alanine as it is a good substrate, it is available in its deuterated forms, and there is a considerable body of experimental data on its interaction with yeast DAAO [14,21]. These studies were complemented with a second substrate, D-asparagine, with the purposes of (a) demonstrating that the effects are not unique to D-alanine; (b) using a slower-reacting substrate to obtain more accurate data; and (c) assessing the validity of ionization values with a substrate having a different α-amino p$K_a$ (the D-asparagine α-amino p$K_a$ is 8.6, compared to 9.7 for D-alanine).

## MATERIALS AND METHODS

### Materials

[2-D]DL-Ala was purchased from CDN Isotopes (Canada). All other materials were purchased from Sigma. Recombinant RgDAAO was expressed and purified from *Escherichia coli* cells as described previously [22]. In order to minimize artifacts arising from changes in buffer composition, pH effects were performed in a poly buffer containing 15 mM $H_3PO_4$, 15 mM Tris, 15 mM $Na_2CO_3$, 250 mM KCl, 1 mM 2-mercaptoethanol, and 1% glycerol. A high KCl concentration was used to buffer against minor changes in ionic strength at different pH values. This buffer was adjusted to the appropriate pH by small additions of HCl or KOH.

### Time resolved stopped-flow spectrophotometry

Kinetic data were acquired in a stopped-flow instrument with a 1-cm path length interfaced to a diode-array detector, as described previously [19,20]. Spectra were recorded in the range of 300–650 nm, with a time constant as low as 0.8 ms per spectrum. Data were acquired from the time of mixing until completion of the reaction. All reactions were measured at 25 °C.

For reductive half-reaction experiments, the stopped-flow instrument was made anaerobic by overnight equilibration with concentrated sodium dithionite solutions. Dithionite was removed prior to experimentation by extensive rinsing with nitrogen-equilibrated buffer. Enzyme solutions were made anaerobic in tonometers by 10 cycles of evacuation and equilibration with oxygen-purged nitrogen. Substrate solutions were made anaerobic by bubbling with nitrogen for at least 10 min in glass syringes. Substrate concentration was varied over a sufficient range to obtain information about both the saturation of observed rates and about $K_{d,app}$. For analysis of observed rate constants, traces of absorbance vs. time were extracted from the spectra vs. time data set. Traces from reductive half-reaction data at 456 and 530 nm were fitted to a sum of exponentials equation to determine observed rate constants using PROGRAM A (from D. P. Ballou, University of Michigan, Ann Arbor, USA). The same program was used to simulate the experimental traces, using a three-step kinetic model (with only the first step reversible), according to Eqn (6), see below. Subsequent analysis of observed rate constants was performed by least-means-squares curve fitting procedures with KALEIDAGRAPH. Rate and dissociation constants were extracted according to the equations of Strickland *et al.* [23]. The deconvolution of the diode-array data was performed using the SPECFIT32 program (Spectrum Software Associates, Chapel Hill, NC, USA).

Enzyme-monitored turnover experiments [24] were performed with air-equilibrated solutions at 25 °C. In brief, the area described by the experimental curve is proportional to the concentration of the limiting substrate. During analysis, this area is divided into segments along the time axis. For each segment a velocity is calculated at the corresponding concentration of remaining limiting substrate. Data traces at 456 nm were analyzed with KALEIDAGRAPH using published equations [24]. Oxygen was the limiting substrate. The concentration of the reducing substrate (at least five concentrations used) was varied over a sufficient range to give information about both $K_m$ and $k_{cat}$.

### Kinetic isotope effects

Buffer and substrate solutions for solvent KIE studies were prepared by dissolving the appropriate reagents in $D_2O$. The pH of solutions was adjusted by addition of concentrated DCl or NaOD, using the equation pD = meter reading + 0.4 to correct for the activity of $D_2O$ solutions towards the pH electrode [25]. Concentrated enzyme stock solutions in $H_2O$ were diluted into $D_2O$ buffers such that, on average, the final proportion of $D_2O$ was 95%, including correction for the protium content of the buffer components. The reductive half-reaction with D-Ala in $D_2O$, or mixtures of $H_2O$ and $D_2O$, was performed as described above. The stopped-flow instrument was rinsed with small volumes of the appropriate anaerobic $H_2O/D_2O$ buffer prior to use. Reactions were performed at 0.5–37.5 mM D-Ala, final concentrations, to ensure measurement of a saturating reduction rate. Primary KIEs were measured with [2-D]DL-Ala either in 100% $H_2O$ or 95% $D_2O$. As for solvent KIEs, a 0.1–100 mM substrate concentration range was used to ensure saturation of observed rates.

All KIEs in this study were calculated by independently determining values of $k_{red}$ from reductive half-reaction

experiments with the appropriate isotope, and then calculating the ratio of $k_{red}$ values. The SE of multiple KIEs was calculated using the standard formula:

$$SE = \text{value } 1 \times \text{value } 2 \times \sqrt{(\text{error } 1/\text{value } 1)^2 + (\text{error } 2/\text{value } 2)^2}$$

Product release is observed in a separate step. Reversibility of the chemical step is discussed in the text. The net effect of these two factors is that the reverse commitment is effectively zero. The effect of events prior to reduction on the observed KIEs (forward commitment) is discussed in the text.

### Proton inventories

For proton inventory studies, buffer solutions that had been previously adjusted to the appropriate pH were combined together to give the desired mixture of $H_2O$ and $D_2O$. Where nonlinear, pH inventories were fit using Eqn (1) [25]:

$$k_n = k_0[(1 - n) + n\phi_{T1}][(1 - n) + n\phi_{T2}] \quad (1)$$

where $k_n$ is the rate constant in $n$ mole fraction $D_2O$, $k_0$ is the rate constant in $H_2O$, and $\phi_{T1}$ and $\phi_{T2}$ are the isotopic fractionation factors for two protons in movement in the transition state having fractionation factors of 0.4 each. The isotopic fractionation factors for a particular site correlate with the isotopic free-energy difference at that site. According to [25], the isotope effect is the ratio of a product over all initial-state fractionation factors to a product over all final-state fractionation factors.

### Interpretation of pH effects

The effect of pH on kinetically relevant parameters involving enzyme–ligand complexes can be described according to the conventions of Dixon [26] and Cleland [27,28].

$$K_d = (K_{d1}\cdot[H^+] + K_{a1}\cdot K_{d2})/([H^+] + K_{a1}) + (K_{a2}\cdot\Delta K_{d2})/([H^+] + K_{a2}) \quad (2)$$

$$K_d = K_{d,acidic} + (1 + 10^{pH - pKa1,(EorS)}) - (1 + 10^{pH - pKa1,(E-S)}) + (1 + 10^{pH - pKa2,(EorS)}) - (1 + 10^{pH - pKa2,(E-S)}) \quad (3)$$

$$Y = (k_{AH}[H^+] + K_a\cdot k_{A-})/([H^+] + K_a) \quad (4a)$$

$$Y = (k_{AH1}[H^+] + K_{a1}\cdot k_{A-1})/([H^+] + K_{a1}) + (K_{a2}\cdot\Delta k_{A-2})/([H^+] + K_{a2}) \quad (4b)$$

$$Y = (K_{a1}\cdot k_{A-1})/([H^+] + K_{a1}) + (K_{a2}\cdot\Delta k_{A-2})/([H^+] + K_{a2}) \quad (4c)$$

Equation (2) describes a situation in which two ionizations affect but do not eliminate binding: $K_{d1}$ and $K_{d2}$ are the two binding constants at low and intermediate pH and $\Delta K_{d2}$ represents the pH dependent modification of the latter; $K_{a1}$ and $K_{a2}$ are the two p$K_a$ values linking the three binding states. Equation (3) is the Dixon equation for a similar situation wherein each curvature in a p$K_d$ vs. pH plot corresponds to an ionization, downward curvature of free E or S (p$K_a$, E or S), and upward curvature of the E–S complex (p$K_a$, E–S) [26]. In Eqn (4) Y is the y-variable (e.g. $k_r$ or $k_{red}$), in Eqn (4a) (single ionization) the term $k_{AH}$ is the value of the rate constant at low pH (protonated form) and $k_{A-}$ is the value of the same rate constant at high pH (unprotonated form). In Eqn (4b) (two ionizations), the term $k_{AH1}$ is the value of the rate constant at low pH (protonated form), $k_{A-1}$ is the value of the same rate constant at high pH (unprotonated form) for the first ionization, and $\Delta k_{A-2}$ is the increase of the same rate constant at high pH (unprotonated form) following the second ionization.

The subscripts 1 and 2 in Eqns (2, 3 4b, and 4c) refer to the first and second ionizations, respectively. Equation (4a) is for a situation when $k_{obs}$ is modified but not eliminated by the ionization [29]. Equation (4b) is a modified version of Eqn (4a) containing two p$K_a$ values. Equation (4c) involves two p$K_a$ values but no plateau at low pH. Only in the case of Eqn (4c) (first ionization) is a proton taken up or released by a group directly involved in the measured parameter. Regression analyses were also carried out using the logarithmic forms of equations 1–3 and yield essentially the same results.

## RESULTS

### Spectral course of the reaction with D-alanine and D-asparagine

The spectral changes accompanying the anaerobic reaction with a ≈500-fold excess of substrate occur in two phases, $k_{obs1}$ and $k_{obs2}$, involving a well defined intermediate, as shown in Fig. 1 for the reaction with [2-D]D-Ala at pH 8. While the rate of the first phase, $k_{obs1}$, is strongly dependent on the substrate concentration, the second shows little dependence. Binding of substrate to form the $E_{ox}$–S complex does not result in measurable spectral effects. The first of the two observed phases is reduction of enzyme-bound, oxidized FAD ($E_{ox}$, Fig. 1, trace 1) to form the reduced enzyme–iminopyruvate complex ($E_{red}$–P, trace 2), which is characterized by the low intensity, long wavelength charge-transfer band maximal around 500 nm [21]. The second phase, $k_{obs2}$, corresponds to the decay of this complex to form fully reduced, uncomplexed enzyme ($E_{red}$, trace 3). In the presence of the second substrate, oxygen, (i.e. under turnover conditions) the enzyme spectrum reflects the oxidized state during the steady-state phase because the rate of oxidation is greater than the rate of reduction. When most of the oxygen is consumed (Fig. 2), $E_{ox}$ is converted rapidly to $E_{red}$–P and $E_{red}$. These spectral changes provide the basis for the experiments described below.

### Enzyme-monitored turnover with D-alanine and D-asparagine

Steady-state studies with these substrates were conducted to complement the measurements of single steps in the reductive half-reaction described below. They were perfomed in

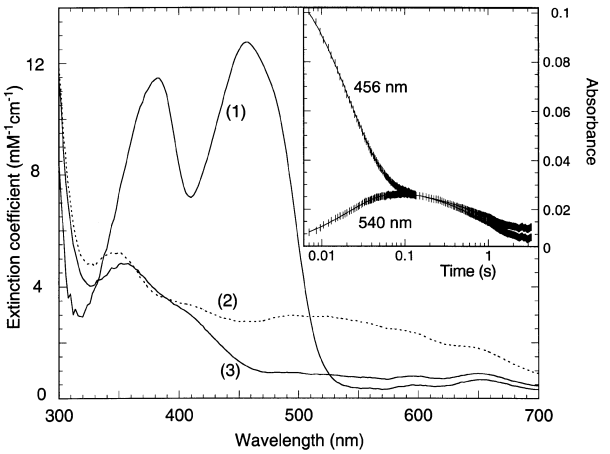


**Fig. 1. Absorbance spectra of species detected in the reaction of RgDAAO with D-alanine at pH 8.0, and time course.** The enzyme, 9.5 μM, was reacted in the stopped-flow instrument with 5 mM [2-D]D-Ala (final concentrations), at 25 °C. Spectra (120) were recorded at intervals of 1 ms up to 120 ms, and 100 spectra thereafter up to 3.2 s using a J & M diode array photometer. The spectra shown are those calculated with the deconvolution program SPECFIT32 for: starting enzyme, $E_{ox}$, (2) the reduced enzyme-iminoacid intermediate, $E_{red}$~P and (3) the final product, free, reduced enzyme, $E_{red}$. (3) The three species shown are at 100% concentration. The inset shows a representative time course for a fast reaction with a $t_{1/2} < 20$ ms (|) are the data points at 455 and 540 nm for the reaction of the enzyme at the same concentration and pL 8.0, in 33% $D_2O$ with 5 mM [2-H]D-Ala. The lines (–) are the fits obtained using a two exponential decay algorithm yielding $k_{obs1} = 112\ s^{-1}$ and $k_{obs2} = 0.7\ s^{-1}$. The vertical bars (|) represent the data points, with no significance to their height.

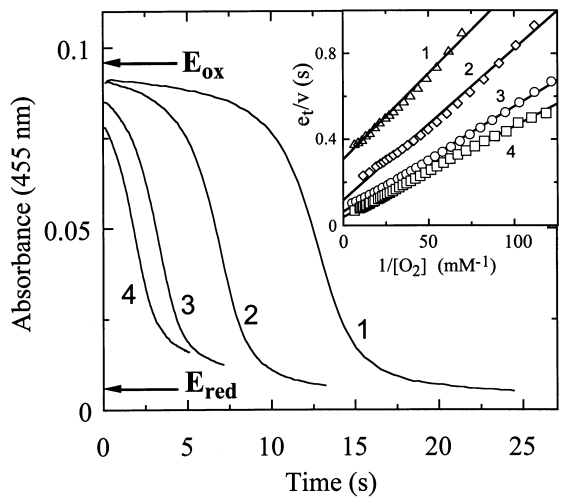


**Fig. 2. Turnover of RgDAAO with D-alanine in $D_2O$ at pH 8.5.** The traces were obtained using the stopped-flow instrument and analyzed according to Gibson et al. [24]. The enzyme, 8.3 μM, was reacted with (1) 0.5 mM, (2) 1.25 mM, (3) 2.5 mM, and (4) 5 mM [2-H]D-Ala (all final concentrations) at 25 °C and 0.253 mM initial $[O_2]$. The course of the reaction was monitored at 455 nm. Inset: Lineweaver–Burk plot of the primary data. The data points were obtained using up to 100 absorbance values from the traces shown in the main graph at fixed time intervals (from 0.247 $s^{-1}$ to 0.051 $s^{-1}$).

$H_2O$ or $D_2O$ at various pL (H or D) values using the method of enzyme-monitored turnover [24], which utilizes the spectral changes described above. In $H_2O$ at pH ≥ 7, the time dependence of the reaction traces with D-Ala exhibits a very short steady-state phase, and such primary data are difficult to be evaluated using Gibson's method [24]. Traces from experiments between pH 5 and 7.5 yield $k_{cat}$ values in the range of 40–170 $s^{-1}$ (not shown). On the other hand, measurements in $D_2O$ are slower due to the solvent KIE and easier to evaluate as shown in Fig. 2 for pD 8.5. Steady-state parameters at high and low pH are given in Table 1. Due to the mentioned difficulties, no attempt will be made to interpret solvent KIEs on turnover.

In order to assess the confidence in the rates derived from measurements of the reductive half-reactions below, simulations of turnover reactions were performed (not shown), using the program SPECFIT32, based on Eqn (5):

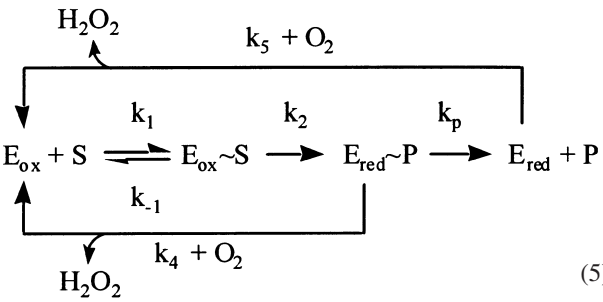


(5)

Compared to single-wavelength data, the use of diode array spectroscopy and analysis with SPECFIT32 has the advantage that the time-dependent concentration of single, occurring species such as ($E_{ox}$ + $E_{ox}$–S), $E_{red}$, and $E_{red}$–P can be followed individually. Reasonable simulations were obtained under the assumption that the spectra of $E_{ox}$ and $E_{ox}$–S are identical, using the spectrum of $E_{red}$–P obtained by deconvolution of reductive half-reaction data with Specfit/32, and using the values listed in Table 2 as well as $k_4 = 1.0 \times 10^7\ M^{-1}{\cdot}s^{-1}$ and $k_5 = 3.0 \times 10^6\ M^{-1}{\cdot}s^{-1}$ determined previously [21]. This method is very sensitive to the accuracy of the input rate constants; error is propagated with each simulated turnover cycle. These successful simulations of turnover data using rate constants from reductive half-reaction data strongly support the accuracy of the reported values.

## pH dependence of turnover parameters

The pH profiles of the parameters $k_{cat}$, $k_{cat}/K_m$, and $K_m$ can yield important information about ionizations relevant to catalysis as discussed by Dixon [26] and Cleland [27,28]. All these parameters for the substrates D-Ala, D-Asn, and $O_2$ show marked pL (pH or pD) dependencies; those for $k_{cat}$ and $k_{cat}/K_m$ reach plateaus at high and low pH as shown in Fig. 3. The data are fit using Eqn (4a) (one ionization, activity plateau at low and high pH). $K_{m,O2}$ and $K_{m,D\text{-}ala}$ behave analogously (not shown, data in Table 1). An interpretation of the pH-dependence of these latter terms, however, will not be attempted in the context of this work. With D-Asn, $k_{cat}$ is lower than $k_{red}$ (Table 3, see also below) at all pH values indicating that the latter is only partially rate limiting in catalysis. With D-Ala in $D_2O$ $k_{cat}$ is three and

**Table 1. Steady state parameters for the reaction of RgDAAO with D-alanine and D-asparagine at various pL values (L = H or D).** See text, Figs 3,7, and 8 and Table 2 for details on the determination of the kinetic constants and p$K_a$ values. ND, not determined.

| | pL = 6 | pL = 10 | p$K_a$ |
|---|---|---|---|
| D-Alanine, turnover in $D_2O$ | | | |
| $k_{cat}$ ($s^{-1}$) | 22 ± 2.1 | 156 ± 25 | 7.7 ± 0.4 |
| $K_{m,D\text{-}Ala}$ (M) | 0.052 ± 0.004 | 0.003 ± 0.001 | 7.4 ± 0.5 |
| $k_{cat}/K_{m,D\text{-}Ala}$ ($M^{-1}$ $s^{-1}$) | 760 ± 50 | 47700 ± 2200 | 9.2 ± 0.1 |
| $K_{m,O2}$ (M) | $(7.5 \pm 1.0) \times 10^{-5}$ | $(47 \pm 8.5) \times 10^{-5}$ | 7.5 ± 0.5 |
| D-Asparagine, turnover in $H_2O$ | | | |
| $k_{cat}$ ($s^{-1}$) | 2.0 ± 0.3 | 25.0 ± 3.0 | 7.6 ± 0.3 |
| $K_{m,D\text{-}Asn}$ (M) | 0.030 ± 0.009 | 0.0034 ± 0.0011 | 5.8 ± 0.4 |
| $k_{cat}/K_{m,D\text{-}Asn}$ ($M^{-1}$ $s^{-1}$) | 17.8 ± 7.5 | 7635 ± 130 | 8.4 ± 0.1 |
| $K_{m,O2}$ (M) | $(3.6 \pm 1.0) \times 10^{-6}$ | $(52 \pm 12) \times 10^{-6}$ | ND |

fivefold slower than $k_{red}$, at pD 6 and 10, respectively. This contrasts with the previous finding that $k_{red}$ is rate limiting with D-Ala at pH 8.3 in $H_2O$ [21]. The discrepancy is explained by the different constitution of the two RgDAAO enzymes used. The earlier data from Pollegioni et al. [21] were obtained using native DAAO purified from *R. gracilis* cells. This preparation is a mixture of three holoenzymes arising from *in vivo* differential proteolysis at the C-terminus. The enzyme used in the current work is homogeneous recombinant RgDAAO expressed in *E. coli*, for which reduction is faster and thus not fully rate-limiting. These observations were an incentive to carry out extensive studies of the reductive half reaction, as detailed below.

## Reductive half-reaction with D-alanine and D-asparagine

Reduction was followed in the stopped-flow apparatus and proceeds via the species discussed above and with the spectral changes shown in Fig. 1 (see inset of Figs 1 and 4). The conversion of oxidized enzyme ($E_{ox}$) into the reduced enzyme–product complex ($E_{red}$–P) proceeds through phase $k_{obs1}$, which corresponds to the steps represented by $k_1$ and $k_2$ [Eqn (6) below]. The second phase in reduction, $k_{obs2}$, the release of product from $E_{red}$–P, is represented by $k_p$ in Eqn (6) [21]. Three species are identified at all pH values, corresponding to those depicted in Fig. 1. The extinction coefficient of each species does not change significantly with pH. From this we deduce that the species exist at the same ionization states at all three pH values; e.g. both $E_{red}$–P and free $E_{red}$ contain $FAD_{red}H^-$ and iminopyruvate is in the protonated ($\alpha C{=}NH_2^+$) form.

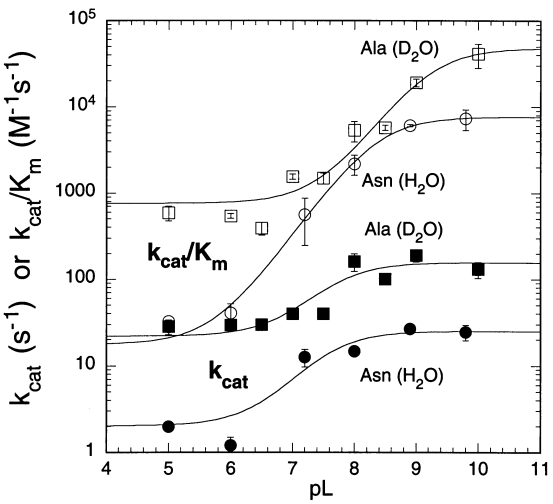


**Fig. 3. pH dependence of $k_{cat}$ (closed symbols) and $k_{cat}/K_m$ (open symbols).** The data were determined for [2-H]D-Ala (squares) in $D_2O$ and for [2-H]-Asn in $H_2O$ (circles) and were obtained according to Gibson [24]. Traces (–) are the fits to the data points using Eqn (4a). The fits yield the following values (p$K_a$ values are reported in Table 1): $k_{cat}$: [2-H]D-Ala, 22 ± 21 and 156 ± 25 ($R^2 = 0.777$); [2-H]-Asn, 2 ± 2 and 25 ± 3 ($R^2 = 0.930$). $k_{cat}/K_m$: [2-H]D-Ala, 760 ± 580 and 48000 ± 2200 ($R^2 = 0.993$); [2-H]-Asn, 18 ± 76 and 7600 ± 130 ($R^2 = 0.999$).

Consistent with the presteady-state mechanism previously described for RgDAAO [21] and for pkDAAO [30], the process observed with D-Ala can be described by the following minimal mechanism, where $k_2$ and $k_p$ are, respectively, the rate constants for enzyme reduction and product release (Eqn 6):

$$E_{ox} + S \underset{k_{-1}}{\overset{k_1}{\rightleftharpoons}} E_{ox} - S \underset{(k_{-2})}{\overset{k_2}{\rightleftharpoons}} E_{red} - P \underset{(k_{-p})}{\overset{k_p}{\rightleftharpoons}} E_{red} + P \qquad (6)$$

As discussed recently by Fisher and Saha [31], the interpretation of KIEs and the assessment of their magnitude is dependent on the presence and magnitude of reversible steps connected with those sensitive to isotopic substitution, in the present case $k_2$ (Eqn 6). Flavin reduction, represented by $k_2$ in the forward direction, is practically irreversible, although the reverse rate constant $k_{-2}$ does have nonzero values. Studies with RgDAAO and pkDAAO using D-Ala and D-phenylglycine as reductants [14,21] indicated that $k_{-2}$ is $< 0.1\%$ of $k_2$. Thus, flavin reduction will be considered irreversible in the analysis here, a situation similar to that encountered by Porter and Bright with L-amino acid oxidase (LAAO) [32]. Product dissociation from $E_{red}$–P into the free keto acid and $NH_4^+$, step $k_p$, is also practically irreversible [21]. This reaction is directly observed in $k_{obs,2}$, a step distinct from flavin reduction. (During turnover $E_{red}{\sim}P$ is oxidized by molecular oxygen and product release proceeds from the (re)oxidized enzyme at a rate much faster than $k_p$ [21]). Together, these factors indicate there is no suppression/diminution of KIEs by reverse commitments.

The velocities of $k_{obs1}$ of the reductive half-reactions at pH 8 and at higher substrate concentrations approach the resolution of the stopped-flow instrument, similar to the case

**Table 2. Kinetic parameters for the reductive half-reaction of RgDAAO with D-alanine and D-asparagine (in parenthesis) at various pL values (L = H or D).** The 'observed' values are the parameters determined from the analysis of the experimental traces at 455 nm and 530 nm, the 'from simulation' values are the parameters determined by simulation of the experimental traces using PROGRAM A (see text for details). $k_r$ is the reciprocal of the slope from the double reciprocal plot of the rate of flavin reduction vs. the substrate concentration.

| | | [2-H]D-alanine | | | | [2-D]D-alanine | | | |
|---|---|---|---|---|---|---|---|---|---|
| | | $H_2O$ | | $D_2O$ | | $H_2O$ | | $D_2O$ | |
| pL | Parameter | Observed | Simulation | Observed | Simulation | Observed | Simulation | Observed | Simulation |
| 6.0 | $k_1$ ($M^{-1}\cdot s^{-1}$) | | 4000 | | 1300 | | 4000 | | 1300 |
| | $k_r$ ($M^{-1}\cdot s^{-1}$) | 5400 ± 200 (23 ± 5.7) | | 880 ± 100 | | 1100 | | 300 | |
| | $k_{-1}$ ($s^{-1}$) | | 300 | | 80 | | 300 | | 80 |
| | $K_{d,app}$ (mM) | 58 ± 16 (23 ± 5.7) | 160 | 120 ± 55 | 144 | 32 ± 4 | 90 | 41 ± 18 | 75 |
| | $k_{red}$ ($s^{-1}$) | 310 ± 50 (2.5 ± 0.1) | 350 | 102 ± 32 | 100 | 35 ± 1.5 | 60 | 12 ± 3.5 | 14 |
| | $k_p$($s^{-1}$) | 1.2 ± 0.5 | 0.7 | 0.6 ± 0.04 | 0.6 | 0.92 ± 0.13 | 0.8 | 0.76 ± 0.14 | 0.7 |
| 8.0 | $k_1$ ($M^{-1}\cdot s^{-1}$) | | 30000 | | 30000 | | 30000 | | 30000 |
| | $k_r$ ($M^{-1}\cdot s^{-1}$) | 32000 (540 ± 48) | | 24000 | | 10000 | | 5600 | |
| | $k_{-1}$ ($s^{-1}$) | | 500 | | 500 | | 1000 | | 1000 |
| | $K_{d,app}$ (mM) | 16 ± 3 (28 ± 5.2) | 35 | 14 ± 9.5 | 28 | 40 ± 1.7 | 45 | 37 ± 9 | 40 |
| | $k_{red}$ ($s^{-1}$) | 510 ± 50 (15 ± 4.2) | 550 | 330 ± 77 | 350 | 430 ± 13 | 350 | 200 ± 26 | 210 |
| | $k_p$($s^{-1}$) | 2.3 ± 0.35 | 2.3 | 1.1 ± 0.1 | 1.1 | 0.97 ± 0.15 | 0.8 | 0.75 ± 0.2 | 0.7 |
| 10.0 | $k_1$ ($M^{-1}\cdot s^{-1}$) | | 150000 | | 150000 | | 150000 | | 150000 |
| | $k_r$ ($M^{-1}\cdot s^{-1}$) | 110000 ± 2000 (4500 ± 1180) | | 95000 | | 43000 | | 71900 | |
| | $k_{-1}$ ($s^{-1}$) | | 500 | | 500 | | 1000 | | 1000 |
| | $K_{d,app}$ (mM) | 8 ± 1.2 (28 ± 14) | 8.7 | 6 ± 2 | 8.3 | 7.8 ± 2.8 | 9.3 | 4.9 ± 1.7 | 8.8 |
| | $k_{red}$ ($s^{-1}$) | 900 ± 130 (130 ± 21) | 800 | 760 ± 30 | 750 | 400 ± 21 | 390 | 320 ± 75 | 320 |
| | $k_p$($s^{-1}$) | 10 ± 2.4 | 8.0 | 4.3 ± 1.3 | 3.0 | 8.4 ± 1.0 | 8.0 | 3.4 ± 0.4 | 3.0 |

**Table 3. Ionizations deduced from pL dependence (L = H or D) of kinetic parameters for the reductive half-reaction of RgDAAO with D-alanine and D-asparagine.** $k_{red}$ ($s^{-1}$) is the rate of flavin reduction obtained at infinite substrate concentration; $k_r$ is the reciprocal of the slope of the double reciprocal plot of the rate of flavin reduction vs. the substrate concentration. $K_{d,app}$ and $pK_a$ values are apparent ones. Except where noted, values were determined as described in the text and figures from fits listed in the Methods section.

| | $pK_{a1}$ | $pK_{a2}$ |
|---|---|---|
| D-Alanine, reductive half-reaction in $H_2O$ | | |
| $k_{red}$ ($s^{-1}$) | 5.7 ± 0.3 | 8.35 ± 0.15 |
| $K_{d,app}$ (M) | 6.45 ± 0.25 | (9.3 ± 3.6) |
| $k_r$ (= $k_{red}/K_{d,app}$) ($M^{-1}\cdot s^{-1}$) | 7.0 ± 0.1 | 9.0 ± 0.1 |
| D-Alanine, reductive half-reaction in $D_2O$ | | |
| $k_{red}$ ($s^{-1}$) | 5.85 ± 0.6 | 8.3 ± 0.1 |
| $K_{d,app}$ (M) | 6.6 ± 0.1 | |
| $k_r$ (= $k_{red}/K_{d,app}$) ($M^{-1}\cdot s^{-1}$) | 7.5 ± 0.2 | 9.5 ± 0.15 |
| D-Asparagine, reductive half-reaction in $H_2O$ | | |
| $k_{red}$ ($s^{-1}$) | 7.7 ± 0.4 | 10.1 ± 0.4 |
| $K_{d,app}$ (M) | 5.9 ± 0.3 | 6.9 ± 0.2 |
| $k_r$ (= $k_{red}/K_{d,app}$) ($M^{-1}\cdot s^{-1}$) | 7.45 ± 0.2 | 9 (fixed) |

reported by Porter & Bright for LAAO [32]. Values for $k_{obs}$ were estimated from the absorbance changes at 455 nm and 530 nm vs. time using PROGRAM A and from global spectral deconvolution analysis using SPECFIT32. To validate the values determined for rates $> 50\ s^{-1}$, a comprehensive deconvolution of the spectra was performed using the SPECFIT32 program. For the cases in which $k_{obs} > 100\ s^{-1}$ or $k_{obs1} \approx k_{obs2}$, it was useful to use the spectrum of the intermediate $E_{red}$–P (see trace 2 in Fig. 1) as a fixed parameter in the fitting routines and as indicated in the instructions for SPECFIT32. This global analysis obtained results of superior reliability to those from fits to traces at individual wavelengths. However, both analyses gave observed rates in excellent agreement. Values for observed rates were verified by extensive simulations of the experimental data for the reactions at pH 6, 8, and 10, with all isotopes used. Simulations were based on the sequential mechanism of Eqn (6) (i.e. a system including steps $k_1$, $k_{-1}$, $k_2$, and $k_p$) and on the extinction coefficients obtained from the deconvolutions. Simulations were performed using either PROGRAM A for single wavelength traces or globally with SPECFIT32 using complete sets of time-resolved spectra in the range 300–700 nm. Experimental and simulated data from single wavelength traces at 455 nm are compared in Fig. 4 and demonstrate a reasonable correspondence at each concentration and pH. The parameters obtained from fitting and used for simulations are listed in Table 2 and in the legend to Fig. 4.

Examples are shown of the concentration dependence of $k_{obs1}$ with D-Ala at pH 6.0, 8.0, and 10.0 (Fig. 5). For the model in Eqn (6), plots such as those in Fig. 5 display $k_{red}$ as the value to which $k_{obs}$ extrapolates at high substrate concentration [23]. This extrapolated value will be referred to as $k_{red}$. Whereas $k_2$ is the discrete rate constant for enzyme reduction/substrate oxidation, $k_{red}$ is the apparent rate constant for reduction and may have contributions from steps other than $k_2$. Saturation is not evident at pH 8 and,

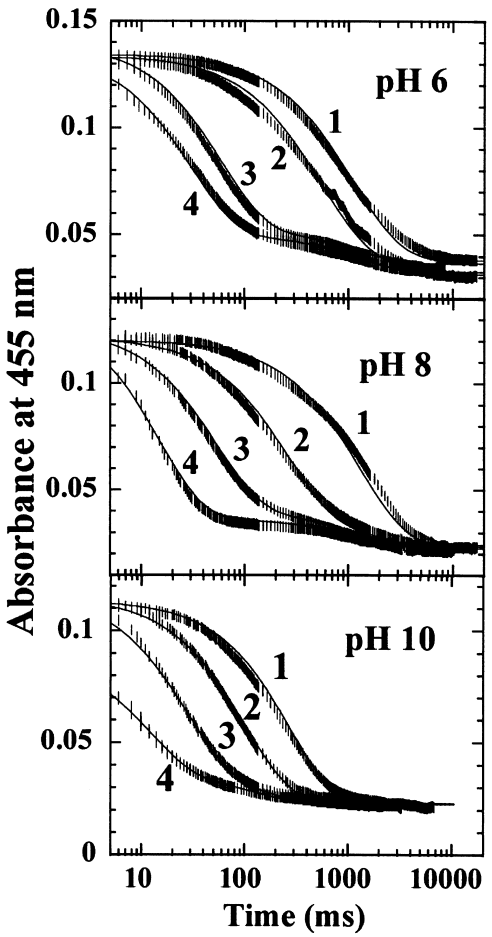


**Fig. 4. Time courses and simulations from the anaerobic reduction of RgDAAO with [2-D]D-alanine at various pH values.** Enzyme was mixed anaerobically in the stopped-flow instrument with the given concentrations of [2-D]D-Ala. The vertical bars (|) represent the data points, with no significance to their height. The solid lines represent simulations using PROGRAM A with a three-step model based on Eqn (6) and the given rate constants. The following extinction coefficients were used for traces simulated at 455 nm: $E_{ox}$ and $E_{ox}$–S = 12600 $M^{-1}\cdot cm^{-1}$, $E_{red}$–$P$ = 4500–4750 $M^{-1}\cdot cm^{-1}$, $E_{red}$ = 2700–3200 $M^{-1}\cdot cm^{-1}$. pH 6.0, 10.7 μM RgDAAO, [2-D]D-Ala concentrations: (curve 1) 1.0 mM, (curve 2) 5 mM, (curve 3) 37.5 mM, and (curve 4) 100 mM. For simulations: $k_1$ = 4000 $M^{-1}\cdot s^{-1}$, $k_{-1}$ = 300 $s^{-1}$, $k_2$ = 60 $s^{-1}$, $k_p$ = 0.8 $s^{-1}$. pH 8.0, 10.3 μM RgDAAO, [2-D]D-Ala concentrations: (curve 1) 0.125 mM, (curve 2) 0.5 mM, (curve 3) 2.5 mM, and (curve 4) 10 mM. For simulations: $k_1$ = 30000 $M^{-1}$ $s^{-1}$, $k_{-1}$ = 1000 $s^{-1}$, $k_2$ = 350 $s^{-1}$, $k_p$ = 0.8 $s^{-1}$. pH 10.0, 9.2 μM RgDAAO, [2-D]D-Ala concentrations: (curve 1) 0.1 mM, (curve 2) 0.3 mM, (curve 3) 1 mM, and (curve 4) 2.5 mM. For simulations: $k_1$ = 150000 $M^{-1}\cdot s^{-1}$, $k_{-1}$ = 1000 $s^{-1}$, $k_2$ = 390 $s^{-1}$, $k_p$ = 8 $s^{-1}$.

thus, $k_{red}$ data obtained by extrapolation have a considerable margin of error. However, the double reciprocal plot of the same data indicates a positive $y$-intercept (Fig. 5, insets). The rate constants obtained from fits of these data (see above) were the starting points for obtaining the constants used in the simulation of the experimental traces, as discussed above. The values of $k_1$ and $k_{-1}$ obtained from the simulations are reliable estimates of the lower limits of these constants, they were also used successfully to simulate the turnover data (see above).

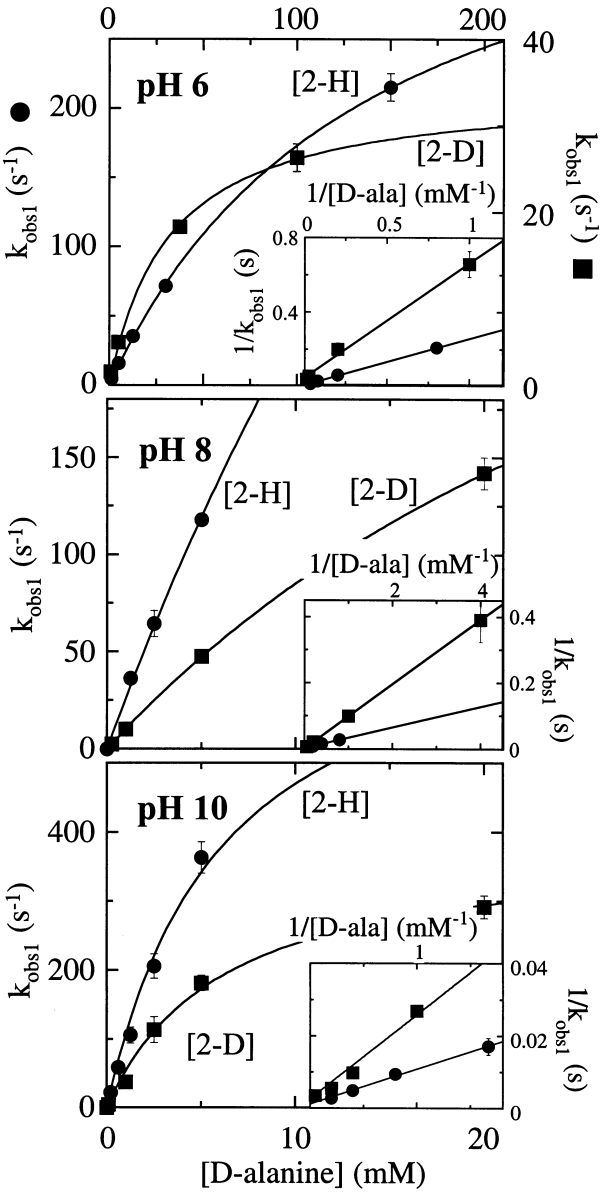


**Fig. 5. Dependence of the observed rate of enzyme flavin reduction $k_{obs1}$ on [2-H]D-alanine (●) and [2-D]D-alanine (■) concentration at pH 6.0, 8.0, and 10.0 in $H_2O$.** Insets: double reciprocal plots of the data reported in the main graph. Vertical bars in all panels indicate ± SE from at least five determinations.

In the reductive half-reaction with D-Asn, the oxidized enzyme species ($E_{ox}$, see Fig. 1, trace 1) is transformed monophasically to a species with the spectrum of uncomplexed, reduced enzyme, $E_{red}$ (not shown, compare to Fig. 1, trace 3). No intermediates were observed at the pH values used. This notable difference, compared to the behavior with D-Ala, indicates that product dissociation ($k_p$, Eqn 6) is faster than reduction or does not affect spectral properties of the species involved. Figure 6 demonstrates the monophasic course of flavin reduction for selected D-Asn concentrations at pH 8.0. Generally, $k_{obs}$ values for D-Asn are much smaller compared to D-Ala, and saturation behavior is evident throughout the whole pH range. Data were analyzed as with D-Ala to determine kinetic constants whose pH dependence is discussed below.

## PH dependence of the reductive half-reaction data

The pH dependencies of the rates of flavin reduction $k_{red}$ with D-Ala and D-Asn are depicted in Fig. 7A. With D-Ala $k_{red}$ is small at low pH, it increases with pH reaching an intermediate plateau in the region pH 6–8, and rises further to attain a limiting rate above pH 10. The data can be fit to Eqn (4b) (finite values for $k_2$ at high and low pH and two p$K_a$ values) or to Eqn (4c) (finite values for $k_2$ at high pH, two ionizations, and a decrease of $k_{obs}$ with a unit slope at low pH). Fits with Eqn (4b) are marginally better, compared to Eqn (4c), however, they are decisively superior to corresponding fits based on Eqn (4a) (one ionization). With D-Asn the data can be fit to equations based on either one (Eqn 4a) or two ionizations (Eqn 4b,c), the second set being somewhat better. The plateau at low pH is particularly evident in this latter case. Values from fits are given in the legend to Fig. 7 and in Table 3.

Figure 7B displays the pH dependence of the term $k_r$ (the reciprocal of the slope of $1/k_{obs}$ vs. 1/[S] from double reciprocal plots, according to Porter & Bright [32]). $k_r = k_1k_2/(k_{-1} + k_2)$ can reduce to $k_2/K_{d,app}$ or to $k_1$ depending on the relative magnitude of $k_{-1}$ and $k_2$. The utility of $k_r$ is that reliable values can be accomplished even when $k_2$ is very fast and saturation of $k_{obs}$ values might not be accurately measured, a concern for the high pH data. The pH dependence of $k_r$ for D-Ala in $H_2O$ or $D_2O$ is analogous to that of $k_{red}$ (compare Fig. 7A,B). With $k_r$ the fits of the D-Ala data indicate a clear preference for the situation where $k_r$ reaches a finite value (plateau) at low pH (Eqn 4b), as opposed to a pH-dependent decrease of $k_r$ with a unit slope (Eqn 4b). With D-Asn the data are also fit best with Eqn (4b) similarly indicating the presence of 2 apparent p$K_a$ values and a plateau at low pH. Values from fits are given in the legend to Fig. 7 and in Table 3. Based on the values

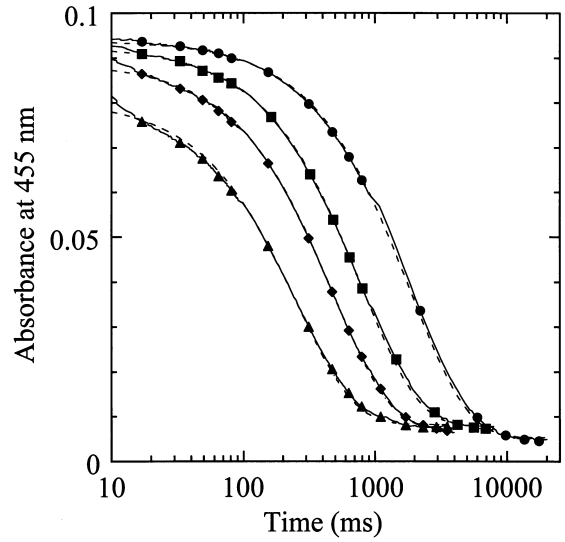


**Fig. 6. Time courses of the anaerobic reduction of RgDAAO by D-asparagine.** RgDAAO, 8.7 μM at pH 8.0, was mixed anaerobically in the stopped-flow instrument with 1.25 mM (●), 2.5 mM (■), 5 mM (◆), and 12.5 mM (▲) D-Asn (all final concentrations), and the changes in absorbance were followed at 455 nm. The points and the continuous lines represent the experimental data, the dashed lines represent the corresponding best fits obtained using a single exponential algorithm.

obtained from simulations of the experimental traces (see Table 2), the lowest limit of $k_{-1}$ approaches the value of $k_2$ from above but is never smaller than it at all pH values, and therefore $k_r$ never reduces to $k_1$. This situation is different from that described for LAAO by Porter & Bright [32] in which a change in rate-limiting step occurs from $k_1$[S] at high pH to $k_2$ at low pH.

Apparent $K_d$ values were obtained from the reciprocal of the abscissa intercept in the double-reciprocal plots of $k_{obs}$ vs. substrate concentration (Fig. 5, insets), or from fits to direct plots such as shown in Fig. 5 according to [23]. Because at first approximation, $K_d = (k_2 + k_{-1})/k_1$, $K_{d,app}$ corresponds to the true $K_d$ ($= k_{-1}/k_1$) only when $k_{-1} \gg k_2$. The pH dependence of $K_{d,app}$ is depicted in Fig. 8. The data can be fit to Eqn (2) and this indicates two ionizations (pH $\approx$ 6.5 and $\approx$ 9) for D-Ala. With D-Asn the pH dependence (not shown) reflects a p$K \approx 6$ (a second p$K_a$ at higher values can be inferred, however, as with D-Ala in $D_2O$, see Fig. 8, a fit is not possible due to data scatter). The same data for D-Ala can also be analyzed using Eqn (3) according to the

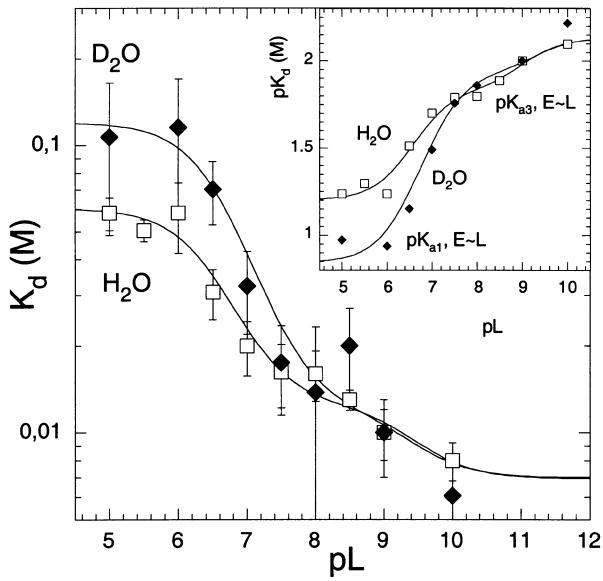


**Fig. 8. pL (L = H, D) dependence of the apparend $K_d$ for D-alanine in $H_2O$ (□) and $D_2O$ (◆).** The data were obtained from plots such as in Fig. 5. The error bars denote the standard deviation for at least 3–5 separate determinations. The line through the data points in $H_2O$ (□) is the fit obtained using Eqn (2), $R^2 = 0.955$. For the data points in $D_2O$ (◆) a fit is not possible due to the large data scatter at pH > 8. The curve was generated using fixed parameters at pH > 7 (those obtained from the fit of the $H_2O$ data) and fitting only for $K_d$ at pH < 7 and p$K_{a1}$. The insert shows the same data, however, analyzed according to Dixon's approach [26] and using Eqn (3). The estimated values are for D-Ala in $H_2O$: p$K_d$ (pH < 6) = 1.2 ± 0.1, p$K_{a1}$ (for E–L) = 6.3 ± 0.2, p$K_{a2}$ (for E or L) = 6.9 ± 0.2, p$K_{a3}$ (for E–L) = 8.9 ± 0.6, and p$K_{a4}$ (for E or L) = 9.2 ± 0.6 ($R^2 = 0.981$). For D-Ala in $D_2O$ the fit trace (–) was obtained similarly as described for the main panel and yields: p$K_d$ (at pH < 6) = 0.8 ± 0.1, p$K_{a1}$ (for E–L) = 6.2 ± 0.1.

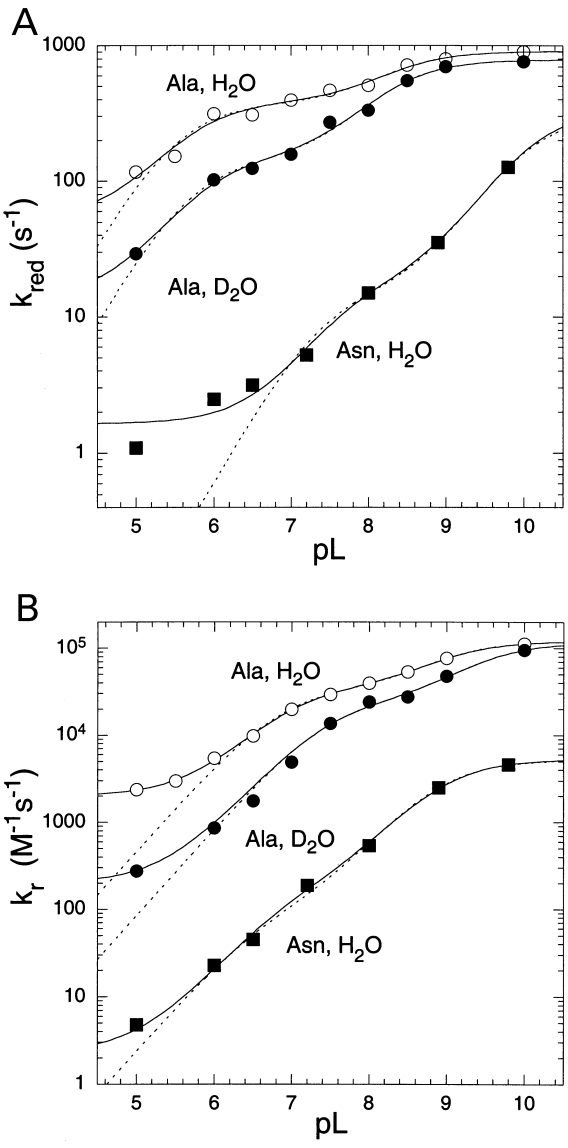


**Fig. 7. pL (L = H, D) dependence of kinetic parameters for the anaerobic reduction of RgDAAO with D-alanine and D-asparagine.** Data were obtained from stopped-flow experiments such as those depicted in Figs 1 and 4 with D-Ala in $H_2O$ (○) and $D_2O$ (●), or with D-Asn (■). (A) Dependence of $k_{red}$, the observed rate of flavin reduction. The lines through the data points are the fit for a finite value at high and low pH with an intermediate plateau using two p$K_a$ values (Eqn 4b), see Table 3. Dashed traces are the fits through the same data points using Eqn (4c), which differs in that $k_{red}$ decreases with unity slope at low pH. The $R^2$ values using Eqn (4b) were 0.990, 0.995, and 0.999 for D-Ala in $H_2O$, D-Ala in $D_2O$ and D-Asn in $H_2O$, respectively. The $R^2$ values using Eqn (4c), were 0.989, 0.994, and 0.990 for D-Ala in $H_2O$, D-Ala in $D_2O$ and D-Asn in $H_2O$, respectively. (B) Dependence of the term $k_r$ ($= k_2/K_{d,app}$, see text). The continuous lines are fits using Eqn (4b), see Table 3. Dashed traces are the fits through the same data points using Eqn (4c), which differs in that $k_r$ decreases with unity slope at low pH. The $R^2$ values using Eqn (4b) were 0.999, 0.997, and 0.997 for D-Ala in $H_2O$, D-Ala in $D_2O$ and D-Asn in $H_2O$, respectively. The $R^2$ values using Eqn (4c) were 0.990, 0.994, and 0.990 for D-Ala in $H_2O$, D-Ala in $D_2O$ and D-Asn in $H_2O$, respectively. Analogous fits of the log of the same data points yield p$K_a$ values within 0.1 units of those from the direct fits. The fits to log values have slightly different profiles due to enhanced weighting of the data at low pH. Fits based on Eqn (4b) are also generally better than those with Eqn (4c) (e.g. $R^2 = 0.984$ vs. $R^2 = 0.971$ for $k_{red}$, Ala in $H_2O$).

conventions of Dixon [26]. This yields four ionizations (Fig. 8, insert), two for E–S, that correspond to those obtained based on Eqn (2), and two for E or S, respectively. While the two values for low pH are reliable, those at pH $>$ 8 are taken as mere indications due to the mentioned problems.

The rate of the second, slow phase $k_{obs2}$ in the reductive half-reaction with D-Ala corresponding to $k_p$ in Eqn (6), is also pH dependent. The value of $k_p$ has a plateau at low pH and reflects a single ionization, $pK_a = 9.3 \pm 0.2$. Experiments addressing the assignment and the mechanistic role of this ionization will be addressed elsewhere [49].

## Solvent isotope effects

The reductive half-reaction with D-Ala at pD 7.5 was measured at 30 min, 4 h, and 8 h after diluting enzyme into $D_2O$ buffer, and in all cases the same reduction rate was observed. From this absence of effects it is unlikely that slow deuterium exchanges on the protein play an adverse role. This was also observed with TvDAAO [14]. A bonus deriving from studies conducted in $D_2O$ is that the lower velocities allow a greater accuracy in the determination of reaction rates. As $k_{red}$ and $k_r$ for D-Ala exhibit a marked dependence both on pL and the solvent $H_2O$ or $D_2O$ (Fig. 7), there is a pL dependence of the solvent KIE on $k_{red}$ and $k_r$ that arises from the ratio of the pH dependence of these parameters in $H_2O$ to those in $D_2O$. This pL dependence for KIEs on $k_{red}$, $k_r$, and $K_{d,app}$ is shown in Fig. 9 along with simulations to Eqn (7).

$$\text{Solvent KIE} = \frac{\text{Eqn }^{H}(4b)}{\text{Eqn }^{D}(4b)} \qquad (7)$$

The values used for the generation of the curves were those obtained from the fits of the data in Fig. 7 (Tables 2 and 3) and are given in the legend to Fig. 9. In order to optimize the simulations, these were modified within the error limits obtained from the fits. This yielded a solvent KIE $\approx 4$ for $k_{red}$ and $\approx 7.3$ for $k_r$ at low pH and KIEs $\approx 1.2$ for both $k_{red}$ and $k_r$ at high pH. The values of $pK_{app1}$ necessary for a good simulation are higher by $\approx 0.2-0.4$ units in $D_2O$ than in $H_2O$, close to the increase in $pK_a$ expected from the equilibrium isotope effect on weak acids [33]. The magnitude of the solvent KIEs on $k_{red}$, calculated from the ratio of $k_{red}$ measured in $H_2O$ to $k_{red}$ extrapolated to 100% $D_2O$, are given in Table 4. This table reports the values at individual pH values, as opposed to those given above from simulations to data in Fig. 9.

The finding of an approximately twofold difference in KIEs for $k_r$ compared to $k_{red}$ is surprising at first. However, the discrepancy can be solved by evaluating the solvent KIE on $K_{d,app}$ (Figs 8,9), which is not a true equilibrium effect but arises from the contribution of $k_2$ in $K_{d,app} = k_1/(k_{-1} + k_2)$. The lower limits for $k_{-1}$ from simulations are sufficiently similar in magnitude to $k_2$ at each pH (Table 2) that no terms drop out of $K_{d,app}$. Any decrease in $k_2$ due to isotopic substitution will result in an increase in $K_{d,app}$ and, hence, an inverse solvent KIE on $K_{d,app}$. Figure 9 shows that the solvent KIE on $K_{d,app}$ becomes less than one, and approaches 0.5 at pH $<$ 8. The term $k_r$ can be represented as $k_2/K_{d,app}$. Therefore, an apparent, inverse solvent KIE on $K_{d,app}$ of $\approx 0.5$ will result in an almost doubling of the KIE on $k_r$. While this analysis involves the assumption that the simulated lower limits of $k_{-1}$ correspond to the actual values of $k_{-1}$, we consider this the simplest, consistent explanation. The validity of this assumption is supported by considering the quotient of $k_r/K_{d,app}$ calculated from the data in Table 2

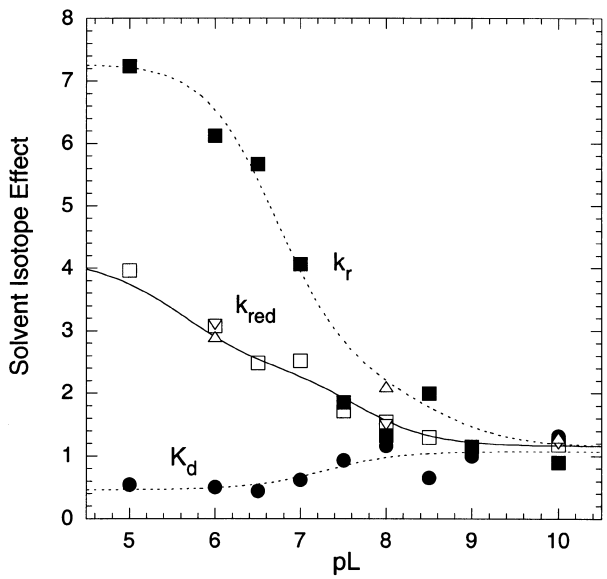


**Fig. 9. pL (L = H, D) dependence of the isotope effect for $k_{red}$, $k_r$ and $K_d$ obtained from the anaerobic reduction with D-alanine.** The data are the ratios of the rates of flavin reduction $k_{red}$ obtained in $H_2O$ to that in $D_2O$ (see Fig. 7). (■): $k_r$ (–) curve obtained by simulation based on Eqn (7) and using the following values for data in $H_2O$ and ($D_2O$): ${}^{H}k_{AH1} = 1600\ M^{-1}\cdot s^{-1}$, ${}^{D}k_{AH1} = 220\ M^{-1}\cdot s^{-1}$, ${}^{H}k_{A\text{-}1} = 25000\ M^{-1}\cdot s^{-1}$, ${}^{D}k_{A\text{-}1} = 10000\ M^{-1}\cdot s^{-1}$, ${}^{H}\Delta k_{A\text{-}2} = 90000\ M^{-1}\cdot s^{-1}$, ${}^{D}\Delta k_{A\text{-}2} = 90000\ M^{-1}\cdot s^{-1}$, $p^{H}K_{a1} = 6.7$ and $p^{D}K_{a1} = 7.2$, $p^{H}K_{a2} = 8.8$ and $p^{D}K_{a2} = 9.0$. (□): $k_{red}$ and (–) simulation curve obtained analogously using: ${}^{H}k_{AH1} = 50\ s^{-1}$, ${}^{D}k_{AH1} = 12\ s^{-1}$, ${}^{H}k_{A\text{-}1} = 335\ s^{-1}$, ${}^{D}k_{A\text{-}1} = 135\ s^{-1}$, ${}^{H}\Delta k_{A\text{-}2} = 575\ s^{-1}$, ${}^{D}\Delta k_{A\text{-}2} = 650\ s^{-1}$, $p^{H}K_{a1} = 5.7$ and $p^{D}K_{a1} = 5.9$, $p^{H}K_{a2} = 7.7$ and $p^{D}K_{a2} = 8.0$. (▽) and (△) are the data for [2-H]D-Ala and [2-D]D-Ala obtained in the solvent inventory experiments (Fig. 10). (●) ${}^{H/D}K_d$ values obtained from primary data as described for Fig. 5. Curve (–) is the fit obtained using a modified Eqn (4a) (single ionization), and reflecting an apparent $pK \approx 7.3 \pm 0.6$.

**Table 4. Deuterium kinetic isotope effects in the reductive half-reaction with D-alanine.** Solvent KIEs are reported as the ratio of $k_{red}$ estimated from extrapolation to saturating [D-Ala] in $H_2O$ to those in $D_2O$ (data as in Fig. 10). Primary substrate KIEs were obtained analogously using [2-H]D-Ala and [2-D]D-Ala (see Fig. 7). The solvent KIE obtained by extrapolation of its pL dependence to values $<5$ is 4.1 (see Fig. 9). The 'multiple' isotope effect is the ratio of $k_{red}$ with [2-H]D-Ala in $H_2O$ to $k_{red}$ with [2-D]D-Ala in $D_2O$. Note that the 'multiple' isotope effects that can be obtained by multiplication of the values determined singularly are similar to those listed in the last row.

| Isotope effect | pL 6 | pL 8 | pL 10 |
|---|---|---|---|
| Solvent, with [2-H]D-alanine | 3.1 ± 1.1 | 1.5 ± 0.3 | 1.2 ± 0.2 |
| Solvent, with [2-D]D-alanine | 2.9 ± 0.8 | 2.1 ± 0.3 | 1.3 ± 0.3 |
| Primary, in $H_2O$ | 9.1 ± 1.5 | 1.2 ± 0.1 | 2.3 ± 0.3 |
| Primary, in $D_2O$ | 8.4 ± 2.4 | 1.6 ± 0.4 | 2.4 ± 0.6 |
| Multiple isotope effect | 26 ± 8.6 | 2.5 ± 0.4 | 2.8 ± 0.8 |

(see also Fig. 7B) which yields $k_{red}$ values quite similar to those determined from fits to the data and shown in Fig. 7A. Consequently, as $k_r \approx k_2/K_d$, it follows that $({}^{H/D}k_r.{}^{H/D}K_{d,app}) \approx {}^{H/D}k_{red}$. At pH $> 8$, the solvent KIE on $k_{red}$ diminishes greatly, and so the ancillary effects on $k_r$ and $K_{d,app}$ approach unity.

In the case of parameters derived from $k_{red}$, p$K_{a1,app}$ for $D_2O$ is shifted by $\approx 0.15$ units higher than the value in $H_2O$, while for p$K_{a2,app}$ the values are similar (Table 3). In the case of $k_r$ (Fig. 7B) both p$K_{a1,app}$ and p$K_{a2,app}$ for $D_2O$ are increased by $\approx 0.5$ units, corresponding to the expected increase [33]. It should be noted that the smaller than expected shifts in the case of parameters derived from $k_{red}$ might result from the relatively large errors in the estimation of p$K_{a,app}$ (0.1–0.6 units, Table 3).

### Proton inventories

Proton inventories were investigated to determine the number and location of exchangeable protons contributing to the solvent KIE. Three different pH values were selected to assess pH-dependent changes in mechanism, and the results are displayed in Fig. 10. At pH 8 and 10, the proton inventories are linear, indicating that the solvent KIE is due to a single site in the transition state. At pH 6, where the solvent KIE is substantially larger, the proton inventory appears to be nonlinear. The pH 6 inventory was fit using Eqn (1) [34]. The isotopic fractionation factors for a particular site correlates with the isotopic free-energy difference at that site. The isotope effect is the ratio of a product over all initial-state fractionation factors to a product overall final-state fractionation factors [25]. The magnitude of the solvent KIEs on $k_{red}$, calculated from the ratio of $k_{red}$ measured in $H_2O$ to $k_{red}$ extrapolated to 100% $D_2O$, are given in Table 4.

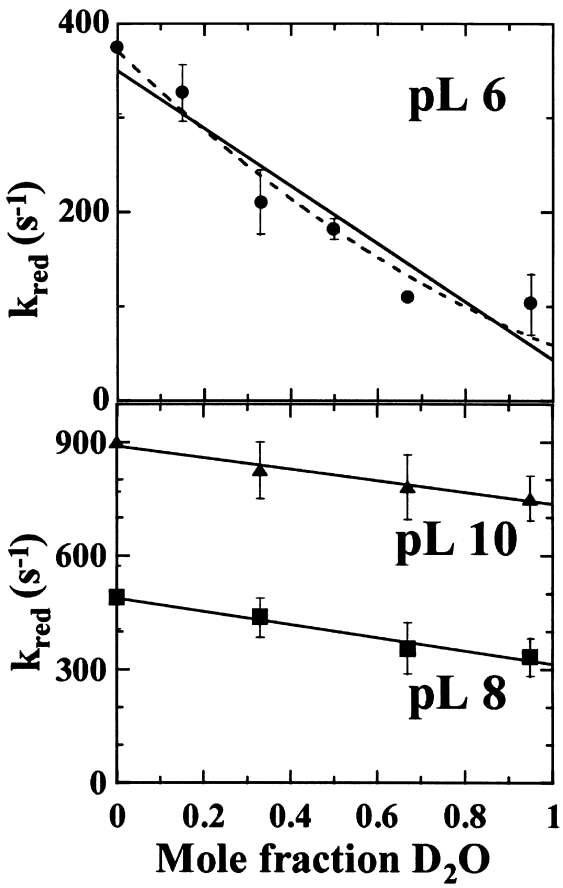


**Fig. 10. Proton inventories for the reduction rate, $k_{red}$, using D-alanine at the pL values shown.** At pL 6, 8 and 10 the experimental data were fit using a linear regression (continuous line). At pL 6 the dashed line represents the fit obtained using Eqn (1) and $\phi_{T1}$ and $\phi_{T2}$ (the isotopic fractionation factors) of $\approx 0.4$ each ($R^2 = 0.955$ vs. $R^2 = 0.906$ using a linear regression).

### Primary substrate kinetic isotope effects

The primary KIE with [2-D]DL-Ala in $H_2O$ was measured to assess the contribution of αC-H bond cleavage to the transition state. As L-amino acids do not inhibit RgDAAO [35], use of the racemic mixture causes no problems. In contrast to [2-H]D-Ala, saturation behavior is evident at all pH values studied using [2-D]D-Ala (Fig. 5). Primary KIE values were calculated as the ratios of the appropriate, observed values of $k_{red}$ (Table 2) and are listed in Table 4. At pH 6, a very large effect of ${}^{H}k_{red}/{}^{D}k_{red} = 9.1 \pm 1.5$ is apparent, consistent with a symmetric transition state in the rupture of the αC-H bond. The primary KIE decreases drastically to $1.2 \pm 0.1$ at pH 8 and is somewhat higher ($2.3 \pm 0.3$ at pH 10). While there is some error in our estimation of $k_{red}$ values at high pH for the reasons mentioned above, these results nevertheless clearly indicate a substantially reduced primary KIE at high pH.

In order to assess the degree of concertedness of the dehydrogenation step, multiple KIE studies were performed, in which the effect of $D_2O$ on the primary KIE also was assessed, and vice versa. As shown in Table 4, the primary KIE is the same when measured in $H_2O$ or $D_2O$. The solvent KIE is also the same when measured with [2-H]D-Ala or with [2-D]D-Ala. This is true at all pL values tested. The observed double KIE at pH 6, i.e. the ratio of $k_{red}$ for [2-H]D-Ala in $H_2O$ to that of [2-D]D-Ala in $D_2O$ is $26 \pm 8.6$ (Table 4), and is clearly multiplicative with respect to the individual KIEs.

## DISCUSSION

### Comparison with similar amino acid oxidases

To our knowledge, five studies have addressed the effect of pH on kinetic parameters of amino acid oxidases. One comprehensive study was carried out by Porter & Bright with ophidian LAAO [32]. A full kinetic analysis, as carried out for LAAO [32] is beyond the scope of the present work. Denu & Fitzpatrick [16,36] addressed the pH dependence of KIEs with pkDAAO. A report of pH effects with RgDAAO [37] will be discussed separately, below. There are important analogies between the pH dependencies of kinetic parameters of RgDAAO, pkDAAO, and LAAO: (a) with all three enzymes, the rate of flavin reduction increases with pH, reflecting apparent p$K_a$ values around 8–9; (b) the primary KIEs decrease with increasing pH. On the other hand, the following differences emerge; with pkDAAO, product release is generally rate limiting in the reductive half-reaction, with RgDAAO it is the reduction step, and

with LAAO and pkDAAO, kinetic parameters ($V/K$) decrease with pH with a unit slope extrapolating to zero [16,32]. With RgDAAO, a plateau at a finite value is attained (Fig. 7 and Table 3). For LAAO, Porter & Bright [32] attributed a p$K_a \approx 9$ to the amino acid α-$NH_2$ group. We reach a similar conclusion in the present work with RgDAAO, as discussed below. Attributions of p$K_a$ values to specific groups has not yet been possible with pkDAAO.

## pH dependencies of catalytic steps

Cleland *et al.* [27,28] discussed the use of pH studies based on the turnover approach to elucidate the mechanism of enzyme-catalyzed reactions. Thus, when both log($k_{cat}$) and log($k_{cat}/K_m$) profiles, such as those shown in Fig. 3 for D-Ala and D-Asn, reflect the same apparent p$K_a$ ($\approx$ 8 in the present case), it is probable that the ionization in question determines which fraction of an E–S complex reacts efficiently to yield product [28]. In the context of the present pH profiles two issues are of paramount relevance. The first is the correspondence of apparent p$K_a$ values, as obtained from plots such as those of Figs 3 and 7, with the microscopic p$K_a$ of an involved functional group. Comparison of the pH profiles in Figs 3 and 7 show that in all cases with D-Ala, an ionization is apparent at pH 8–8.5, while only in the plots of the reductive half-reaction parameters (Fig. 7) a second apparent p$K_a$ of $\approx 6$ is found. The behavior of the plots with D-Asn is analogous, although the curves in Fig. 7 are shifted to higher pH values. The question is therefore whether, and to what extent, these two p$K_a$ values are affected by or result from kinetic artifacts. Cleland [28] refers to profiles such as those shown in Fig. 7 as possessing a 'hollow', and has indicated this can arise from a shift of the apparent p$K_a$ of log($1 + k_2/k_{-1}$). The 'hollow' can have the value of a pH unit or more when a substrate is 'sticky' [28]. As discussed above and indicated in Table 2, $k_{-1} \geqslant k_2$ but not $k_{-1} < k_2$. Consequently, a displacement of $< 1$ pH unit would be expected, while the observed difference between p$K_{a1}$ and p$K_{a2}$ is $> 2$ pH units (Fig. 7). Importantly, such a 'hollow' is not present in the log($k_{cat}$) and log($k_{cat}/K_m$) profiles (Fig. 3), as predicted in the case of 'sticky' substrates [27,28]. Furthermore, the same general behavior is observed with D-Asn, a substrate for which $k_{cat}$ and $k_{red}$ are more than one order of magnitude slower compared with D-Ala, and for which kinetic complications should be less evident. Therefore, we conclude that the p$K_a$ values $\approx 8$ deduced from the plots of Figs 3 and 7 reflect true ionizations, although their absolute values can be altered by kinetic contributions. Based on the same reasoning, we assume that the second apparent p$K_a$ values of $\approx 6$ and $\approx 7.6$ with D-Ala and D-Asn, respectively, also reflect true ionizations.

The second important point is whether the decrease of the parameters with pH leads to a finite value or approaches zero with a unit slope. The plots of the parameters derived from the reductive half-reaction in Fig. 7 suggest a 'plateau', although this interpretation could be debated. In contrast, the pH profiles of log($k_{cat}$) and log($k_{cat}/K_m$) support, unambiguously, the presence of a pH-independent reaction rate at low pH. This indicates that chemical catalysis can proceed without the involvement of an active site base. Thus, the pH dependence of all kinetic parameters with both D-Ala and D-Asn indicates that deprotonation accelerates but is not required for the chemical reaction, and that base catalysis is not essential. This finding is inconsistent with any mechanism in which deprotonation is mandatory for catalysis, such as a carbanion mechanism.

## Catalytic scheme for the reductive half reaction

The kinetic data (Table 2) and the pH dependence of $k_{red}$ depicted in Fig. 7 demand (at least) two distinct kinetic pathways of product formation at pH $>$ 8 (fast) and $<$ 7 (slow) that are operative in parallel at intermediate pH values. A possible scenario has been depicted in Scheme 1. This scheme is similar to one described by Porter & Bright for LAAO [32], although the equilibria and steps leading to the reacting complexes $[E_{ox}-SH^+]^+$ and $[E_{ox}-S^\circ]^\circ$ have been omitted and two paths, $k_2$ and $k'_{2,Hoff}$, leading to product formation are present. An observation relevant to

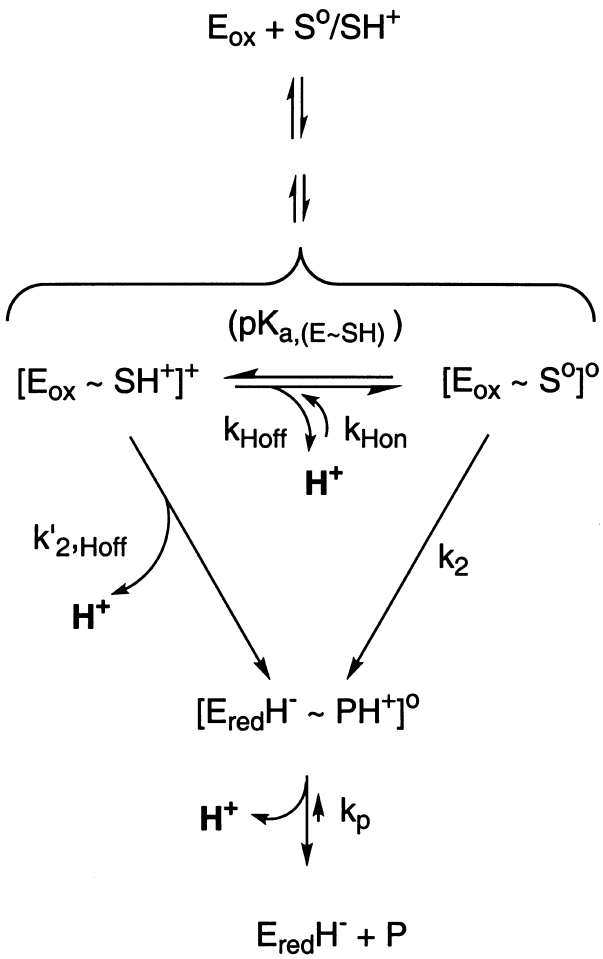


**Scheme 1. pH dependence of the kinetic parameters for the reaction of RgDAAO with D-alanine, at pH values below and above the apparent p$K_a \approx 8$ derived from Figs 3 and 7.** The superscripts denote the net charges of relevant species present at the active site. For simplicity oxidized, uncomplexed enzyme is represented in neutral form ($E_{ox}$), and the charges of Arg285 (positive) and of the substrate carboxylate (negative), which neutralize each other, are not indicated. Thus, $SH^+$ and $S^\circ$ refer to the charge of D-Ala in the neutral (zwitterionic) and anionic forms. $PH^+$ is similarly the neutral (zwitterionic) form of iminopyruvate. Note that $k'_{2,Hoff}$ is the combined step involving flavin reduction and release of $H^+$, see text for details.

the presented mechanism is the complete absence of biphasic behavior in the flavin reduction step $k_{obs1}$ (phase 1 in Fig. 1, inset, corresponding to $k_{red}$) at various pH values, such as those of Figs 1, 4, and 6. This requires that some step(s) interconnecting $[E_{ox}-SH^+]^+$ and $[E_{ox}-S^\circ]^\circ$ to be rapid and $H^+$-dependent (Scheme 1). This is supported by simulations based on corresponding models that indicate that flavin reduction becomes biphasic when any step or combination of steps involved in the equilibration of $[E_{ox}-SH^+]^+$ and $[E_{ox}-S^\circ]^\circ$ is made rate limiting, with the slower phase reflecting the rate of the limiting step(s) (not shown). Furthermore, the extent and ratio of the resulting phases would be dependent on the pH. Note that $[E_{ox}-SH^+]^+$ and $[E_{ox}-S^\circ]^\circ$ can equilibrate through $k_{Hoff}/k_{Hon}$ and also through the steps leading up to formation of the depicted complexes. An analogous situation with similar conclusions has been described by Porter & Bright [32], who worked out the equations and limitations of this type of scheme for presteady-state situations.

While formation of $[E_{red}H^- - PH^+]^\circ$ from $[E_{ox}-S^\circ]^\circ$ via $k_2$ by hydride transfer does not involve particular kinetic problems, two alternative paths are conceivable for the reaction starting from $[E_{ox}-SH^+]^+$. In the first path, $[E_{ox}-SH^+]^+$ first deprotonates via $k_{Hoff}$ to form the intermediate $[E_{ox}-S^\circ]^\circ$, and subsequently $[E_{ox}-S^\circ]^\circ$ produces $[E_{red}H^- - PH^+]^\circ$ via $k_2$. The second path is the conversion of $[E_{ox}-SH^+]^+$ directly to $[E_{red}H^- - PH^+]^\circ$ through the combination of hydride transfer and deprotonation steps in a concerted/synchronous process involving $k'_{2,Hoff}$ (Scheme 1, lower left branch). In this case $[E_{ox}-S^\circ]^\circ$ does not occur as a distinct species or intermediate. The occurrence of the second variant is required by the multiple KIEs (discussed below), indicating a single transition state in the formation of $[E_{red}H^- - PH^+]^\circ$ and by the proton inventories (that show an isotope effect arising from two sites at pH 6 and from one site at pH $\geq$ 8). Scheme 1 also requires $[E_{ox}-S^\circ]^\circ$ to partition between $k_2$ and $k_{Hon}$. At high pH, the net flux through $k_{Hon}$ becomes very small and the rate of flavin reduction approaches the upper limit of $\approx 960\ s^{-1}$ (the value for $k_{A\text{-}1} + k_{AH1} + \Delta k_{A2}$ at high pH, obtained from the fit in Fig. 7A). With lower pH, $k_{Hon}$ will trap $[E_{ox}-SH^\circ]^\circ$ as $[E_{ox}-SH^+]^+$ with increasing efficiency, and consequently the only important reaction path will be the concerted step $k'_{2,Hoff}$ with a limiting rate of $\approx 50\ s^{-1}$ ($k_{AH1}$ low pH, Fig. 7A). Direct support for this coupling comes from studies by Fitzpatrick & Massey [38], who showed that in the anaerobic reaction of pkDAAO with D-Ala, one $H^+$ is released to solvent subsequent to binding of neutral substrate ($SH^+$) and concomitant with flavin reduction (corresponding to $k'_{2,Hoff}$ in this work, Scheme 1). This scheme is in agreement with the observation of a plateau of reactivity at low pH where the rate of $\approx 50\ s^{-1}$ would therefore correspond to $k'_{2,Hoff}$, a pH-independent step. This is in full agreement with the chemical requirement that within $[E_{ox}-SH^+]^+$ the amino acid $NH_3^+$ group must deprotonate for the reaction to occur. Otherwise, the resulting product would contain an imine bearing two positive charges ($>C{=}NH_3^{++}$). The assignment of this ionization to the α-amine will be discussed below. The catalytic relevance of product release (step $k_p$, Scheme 1) and its pH dependence will be addressed elsewhere [49].

## Attribution of ionization constants

We consider the ionization at $pK_a \approx 8$, that is responsible for the significant pH effects with D-Ala (Figs 3 and 7A), to be due to the substrate α-amino group in the $E_{ox}-S$ complex (Scheme 1). The alanine $pK_a = 9.7$ would therefore be lowered by one unit upon binding (see also Fig. 8). This ionization is probably reflected also in the pH dependence of $K_d$ (Fig. 8, Table 3). According to the conventions of Dixon [26] and as outlined in Materials and methods, the directions of curvatures in Fig. 8 (insert) allow the attributions of two apparent $pK_a$ values to $E_{ox}-S$ (6.3 ± 0.2 and 8.9 ± 0.6). The data for the lower value are reliable, while the second ionization at pH $\approx$ 9 is not well defined. The ionization at pH $\approx$ 6.5 that has the major effect on the apparent $K_d$, also exerts a substantial effect on $k_{red}$ (Fig. 7A). The Dixon analysis also indicates two p$K$ values for free species at $\approx$ 6.9 and $>$ 9; the first belongs to free enzyme while the second can be attributed to free alanine. The attribution of the $pK_a \approx 8$ to bound alanine corresponds to that of Porter & Bright for LAAO based on the pL-dependence of $k_r$ [32]. It is also based upon the three-dimensional structure of RgDAAO [15], at the active center of which no functional group possibly having a $pK_a$ in this range is present. In addition, this assignment is most consistent with the pH-dependent change in the proton inventories.

The attribution of the second ionization, corresponding to a $pK_a$ of $\approx$ 6, evident in the plots of Fig. 7, to specific groups is not feasible in the present context. Again, based on the three-dimensional structure of the enzyme active center [15], we have to assume that the functional group modulating this pH dependence is located outside the active site. Apparently, the effects of the two ionizations overlap, rendering a straightforward interpretation difficult. The ionizations listed in Table 3 can be attributed to two groups, $pK_{a1}$, and $pK_{a2}$, with apparent values at $<$ 7 and $>$ 8. These apparent $pK_a$ values probably reflect the same microscopic ionizations discussed above. The variance in values could result from significant but varying kinetic contributions, particularly in the case of those derived from $k_{cat}/K_m$ and $K_{d,app}$ functions.

## Isotope effects

*Primary substrate KIEs*. In analogy to LAAO [32], the KIE for the cleavage of the αC-H bond is high at pH 6 ($\approx$ 9 for RgDAAO vs. 5 with LAAO [32]) and can be assumed to be close to the intrinsic one. At pH 8, the KIE is substantially diminished ($\approx$ 1.5), while it increases somewhat at pH 10 to $\approx$ 2.4 (Table 4). An almost complete suppression of a primary KIE would be surprising for this type of reaction, although different magnitudes of a KIE could be expected for the two pathways depicted in Scheme 1. We interpret the pH-dependent suppression as resulting mainly (but not completely, as the KIE $\approx$ 2.4 at pH 10 is substantial) from a kinetic effect: a plausible, general explanation for such phenomena has been discussed recently by Massey *et al.* [39] to explain the abolition of substrate intrinsic KIEs on observed rate constants that depend on the interplay of rates preceding the step of flavin reduction. Such a kinetic system, as depicted in Eqn (8), consists of that of Eqn (4) with the addition of an equilibrium between the binding ($k_1$, $k_{-1}$) and

the isotope-sensitive, chemical step ($k_2$, $k_{-2}$):

$$E_{ox} + S \underset{k_{-1}}{\overset{k_1}{\rightleftharpoons}} E_{ox} - S \underset{k_{-1a}}{\overset{k_{1a}}{\rightleftharpoons}} E_{ox} - S' \underset{k_{-2}}{\overset{k_2}{\rightleftharpoons}} E_{red} - P \quad (8)$$

This additional step might represent a process such as a two step binding, however, it does not involve any chemical transformations besides uptake/release of $H^+$ ions, as detailed below. Yorita *et al.* [39] have discussed Eqns (9), (10) and (11) that describe the kinetic parameters based on the system of Eqn (8):

$$k_{red} = \frac{k_{1a} \cdot k_2}{(k_{1a} + k_{-1a} + k_2)} \quad (9)$$

$$K_d = \frac{[(k_{-1} \cdot k_{-1a}) + (k_{-1} \cdot k_2) + (k_{1a} \cdot k_2)]}{k_1 \cdot (k_{1a} + k_{-1a} + k_2)} \quad (10)$$

$$(k_r =) \frac{k_{red}}{K'_d} = \frac{k_1 \cdot k_{1a} \cdot k_2}{(k_{-1} \cdot k_{-1a}) + (k_{-1} \cdot k_2) + (k_{1a} \cdot k_2)} \quad (11)$$

In this system the KIE on $k_{red}$ residing intrinsically on $k_2$ is suppressed when $k_2$ becomes $> k_{1a}$, and when $k_{red}$ is not dependent on the bimolecular term $k_1$[S] (Eqn 8). A similar situation is encountered with medium chain acyl-CoA dehydrogenase where an equilibration step analogous to $k_{1a}$, $k_{-1a}$ of Eqn (8) masks the intrinsic isotope effect on substrate reduction with 'fast' substrates [40]. While it is beyond the scope of the present work to discuss in detail these equations and their effect on the KIE on $k_{red}$, simple inspection of Eqn (9) indicates that full expression of the KIE, as is the case at low pH, is expected when $k_2 << k_{1a}$ and $k_{-1a}$. This leads to the unusual situation that there is an increase of $k_{red}$ with pH, which must correspond to a pH dependent increase of $k_2$ concomitant with a decrease of the KIE. Consequently $k_{1a}$ must also increase in a pH-dependent manner, but less so than $k_2$, as from pH $\approx 8$ and upward the KIE is substantially suppressed, i.e. a preceding step such as $k_{1a}$ becomes rate-limiting. Therefore, step $k_{1a}$, $k_{-1a}$ must also be pH-dependent, and its microscopic p$K_a$ might underlay one of the apparent p$K_a$ values resulting from Fig. 7. An analogous inspection of Eqns (10) and (11) suggests intuitively that $k_r$ and $K_d$ will depend on the ratios of involved rate constants that are themselves pH-dependent. The rationalization of the present results based on Eqn (8) also can explain the observation of saturation behavior ($k_1$,$k_{-1} > k_{1a}$,$k_{-1a}$,$k_2$) deduced from the results of Fig. 5, and from simulation experiments. In addition, this model is consistent with the observation of a solvent KIE on $K_{d,app}$ and $k_r$, as mentioned above.

With LAAO, an analogous pH dependence of the primary KIE was found [32], however, it reflected a single ionization. With pkDAAO, Denu & Fitzpatrick [16] reported a reduction from 5.1 at pH 4.0 to 1.2 at pH 10.5 for the $V/K_m$ ratio of D-Ala. The large primary substrate (and solvent) KIEs observed in the current study at pH 6 indicate a symmetric transition state during rupture of the αC-H bond [41]. In particular the data reinforce the contention that pkDAAO, RgDAAO, and LAAO function by the same chemical mechanism. As both hydride transfer and carbanion mechanisms are expected to give rise to a large primary substrate KIE, this finding alone cannot distinguish between these mechanisms.

*Multiple KIEs*. A basic mechanistic question is the discrimination between the occurrence of discrete intermediates or of a single transition state. Multiple KIE experiments (Table 4) can provide information on this issue. In the case of discrete steps, an isotope effect will be diminished by the presence of a second isotope [42,43]. If the reactions are concerted and involve a single transition state, then each isotope effect will be unaffected or possibly enhanced by the presence of the second isotope [42,43]. Stated differently, the KIE calculated by dividing the rate with no isotopic substitution by the rate with both isotopes present (a 'double' KIE) will be the product of the individual KIEs in the case of a completely concerted/synchronous reaction. A multiplicative effect arises from the additive nature of changes in activation enthalpies, ΔH‡, for the modification of two bonds proceeding through a single transition state. Two clear cases of the technique that supported concerted mechanisms are for chorismate mutase-prephenate dehydrogenase [44] and aspartate aminotransferase [45]. In the present case, and at all pH values tested, the solvent isotope effect is clearly the same when measured with [2-H]D-Ala or with [2-D]D-Ala (Table 4). Likewise, the primary substrate

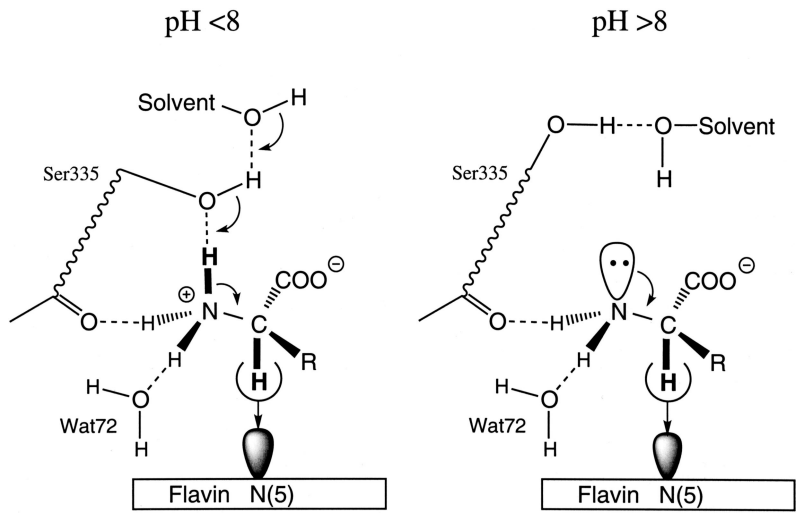


**Scheme 2. Schematic representation of the orientation of flavin, substrate D-alanine, and Ser335 at pH > 8 and pH < 8 and H-bond interactions.** The figure represents the bond alignment required for dehydrogenation of a D-amino acid in an antiperiplanar mode based on the three-dimensional structure of the complex of reduced RgDAAO with D-Ala at 1.2 Å resolution [15]. The position of Ser335 at pH > 8 corresponds to that observed in the three-dimensional structure [15]. At pH < 8, the side chain of Ser335 has been 'rotated' to form a H-bond with the substrate α-ammonium as required for efficient catalysis. The lobe extending from the flavin N(5) represents the LUMO orbital. Note that the difference between the two cases resides in the reaction at low pH requiring concomitant transfer of one $H^+$ to solvent via the intermediacy of Ser335-OH. See text for details.

isotope effect is the same in both solvents. In other words, the 'double' KIE is the product of the primary and solvent KIEs. At pH 6, where the α-amino group of the substrate is protonated, dehydrogenation is coupled with deprotonation of the substrate $\alpha NH_3^+$. At pH $>$ 8, the magnitude of the solvent KIE would be more consistent with a secondary KIE, however, the kinetic effects discussed above do not allow a differentiation between suppression and an intrinsic reduction of the solvent KIE. The solvent KIEs are discussed more thoroughly below. Multiple KIEs have supported concerted mechanisms in the reduction of TvDAAO with phenylglycine [14], and for the α,β-dehydrogenation of acyl-CoA by medium chain acyl-CoA dehydrogenase with α,β-dideutero substrates [46]. Thus, dehydrogenation by RgDAAO or TvDAAO proceeds concertedly with deprotonation at pH $<$ 8 arguing most strongly against the occurrence of discrete intermediates of whatever type. This is fully consistent with the kinetic mechanism discussed above (Scheme 1) in which deprotonation and dehydrogenation are coupled via the step $k'_{2,Hoff}$.

*Solvent KIE'*. Based on its magnitude, we deduce that the fairly large solvent KIE of ≈ 4 (Fig. 9, Table 4) found at pH 6 is a primary one, although it may also include secondary isotope effects originating from the presence of three deuteriums in the $\alpha ND_3^+$ group. Therefore, we attribute this solvent KIE to the cleavage of one of the $\alpha N\text{-}D_3^+$ bonds in the dehydrogenation step. The proton inventories (Fig. 10) are consistent with an isotope effect generated by two exchangeable sites in the transition state at pH 6 and by a single site, located in the transition state, at higher pH values (Scheme 2), i.e. one of the two protons involved at pH 6 ionizes such that it does not contribute to the transition state operative at higher pH, while the second of the two protons is in movement at all pH values studied. This is consistent with the two transition states shown in Scheme 2. The proton involved only at low pH is that responsible for most of the solvent isotope effect at pH $<$ 8. The assignment of this proton to the transition state indicates that there is a hydrogen transfer (as a proton, a hydrogen atom, or a hydride) from an exchangeable site in flight in the transition state for enzyme reduction [34]. In terms of the model in Scheme 2, the concerted reaction of $[E_{ox}{-}SH^+]^+$ to products are consistent with the solvent KIEs if dehydrogenation and deprotonation are highly concerted/synchronous.

Solvent and primary substrate KIEs decrease with increasing pH and reflect the ionization of the (bound) substrate $\alpha NH_3^+$ at $pK_a \approx 8$. The large solvent KIE disappears above this $pK_a$ as the proton responsible for the effect dissociates, leaving only a small, perhaps secondary, solvent KIE at high pH. The change in relative magnitude of $k_{1a}$ and $k_2$, discussed in context of Eqn (8), is proposed to be responsible for suppression of the primary substrate KIE at high pH. Changes in the magnitude of $k_{1a}$ and $k_2$ are likely to occur either as a consequence of the same ionization or of the unidentified ionization at $pK_a \approx 6$. Solvent and substrate KIEs therefore both diminish as a result of differing effects of the same two ionizations.

The single transition state proton responsible for the small solvent KIE (for [2-D]D-Ala: 1.2 ± 0.2 from Fig. 10, and ≈ 1.15 from the extrapolation at high pH of Fig. 9) observed at pL 10 does not ionize over the measured pH range. Interestingly, the same situation was reported for $V_{max}$ with pkDAAO and D-Ala as substrate, where the proton inventories at pH 6 and 10 show a similar behavior [36]. The assignment of this proton to one of two specific substrate hydrogen bonds in the transition state can be tentatively made based on the three-dimensional structure of RgDAAO [15]. The α-amino group of the substrate is linked to the enzyme via two symmetrical, tight hydrogen bonds to Water72 and Ser335=O (2.82 Å each), as depicted in Scheme 2. The third $\alpha NH_3^+$ proton, which would only be present at low pH, must therefore be located at the fourth position of the substrate α-N tetrahedron, as discussed above and shown in Scheme 2 [15]. At pH $>$ 8, this position would be occupied by the $NH_2$ lone pair. While this $H^+$ is the one removed concomitant with hydride transfer and is responsible for the large solvent KIE at pH 6, the remaining two amino protons in Scheme 2 would be expected to give rise to a secondary KIE as the $\alpha\text{-}NH_2$ is converted to $\alpha{=}NH_2^+$ ($sp^3$ to $sp^2$ rehybridization). A secondary KIE would be consistent with the exchangeable nature of the proton and with the proton inventories, indicating the involvement of a transition state proton that does not ionize between pH 6 and 10. Also, the multiple KIE experiments indicate that motion of this proton is coupled with dehydrogenation at the α-carbon. However, two protons, not one, as indicated by the proton inventories, would be expected for such an effect, unless they are not equivalent in the transition state. As there is significant error for the solvent KIE values at pH 8 and 10, a secondary KIE is by no means established by the data and is only offered as a possible explanation. We feel that this is the simplest, reasonable explanation for the presence of a solvent KIE at pH $>$ 8.

## Possible role of Ser335-OH

From the above discussion, the question about the mechanism of transfer to solvent of the $H^+$ released from the $\alpha NH_3^+$ and its mediation becomes relevant, in particular as the three-dimensional structure of RgDAAO [15] shows the absence at the active center of any functional groups capable of essential acid/base catalysis. Furthermore, the three-dimensional structure does not show obvious 'channels' by which this proton might access solvent, although simple movements of protein functional groups or domains (breathing) could be a sufficient alternative for the purpose. In this context, and as suggested previously [15], Ser335-OH, although not in contact with the $\alpha NH_3^+$ group, can form a H-bond with it upon simple rotation around the αC-βC bond. This interaction could therefore facilitate deprotonation of the $\alpha NH_3^+$ [15] in a coupled deprotonation/dehydrogenation step in which a $H^+$ is transferred to solvent. This reaction is likely to proceed with the C-H and the N-H bonds to be broken being in antiperiplanar configuration, as shown in Scheme 2. In LAAO, His223 could perform a similar task [47], where it could act as a true base catalyst, while in pkDAAO, Tyr224 is a candidate [13,17]. As discussed for all of the pH effects above, this possible role for Ser335 is not essential for the reaction to occur.

## Mechanistic conclusion

The effect of pH on the reactions catalyzed by the closely related enzymes pkDAAO and LAAO has been investigated

in depth [16,32,36,37]. For the reaction of pkDAAO with D-Ala, Denu & Fitzpatrick concluded that a group with a p$K_a$ of 8.1 must be deprotonated for activity [16]. They suggested that this group acts as the essential active site base in a carbanion mechanism, an interpretation that cannot be upheld in view of more recent work [13–15,17]. In view of the present results, of the three-dimensional structures of pkDAAO [13,17], RgDAAO [15], and LAAO [47], and in analogy to LAAO [32], it appears reasonable that also with pkDAAO the p$K_a$ in question is that of the substrate α-amino group. The solvent KIE and its pH dependence are consistent with the mechanism proposed by Miura involving hydride transfer from the substrate α-amine [17]. However, the existence of the primary substrate KIE, and more importantly the multiple KIEs, argue against this mechanism as it is difficult to envisage it proceeding in the absence of intermediates.

Severe discrepancies exist between our results and a report dealing with pH effects on catalysis by the same RgDAAO [37]. The pH dependence of $V_{max}/K_m$ reflect two p$K_a$ values at $\approx 6$ and 8 that might correspond to those reported here. However, the shape of the profiles exhibits gross differences such as declining limbs at low and high pH and no plateaus [37]. We are at odds for an adequate explanation for these differences. Denu & Fitzpatrick [36] have interpreted their results, indicating an absence of solvent isotope effects in the reaction of pkDAAO with D-serine, as evidence against a concerted mechanism. This contrasts with reports from Miura *et al.* [12] that the reaction of pkDAAO is concerted. While our results tend to support the second interpretation, a rationalization of the difference with pkDAAO [36] is difficult. We suspect kinetic differences are at the origin of the discrepancy, the kinetic behavior of pkDAAO [1] being even more complicated than that of RgDAAO.

It is interesting to compare the mechanism discussed here with that proposed by Cleland *et al.* for the dehydrogenation of L-Ala by $NAD^+$ catalyzed by alanine dehydrogenase from *Bacillus subtilis* [48]. A hydride transfer mechanism for $NAD^+$ dependent enzymes is generally accepted. Similarities between the flavin and $NAD^+$-dependent systems at the molecular level should be apparent. The pH profiles reported in [48] reflect p$K_a$ values for cationic acids at 7 and 9–9.6, and indicate that alanine reacts with an α-amine in the neutral form. While these ionizations could not be attributed to specific groups in the $NAD^+$-dependent enzyme, a mechanistic correspondence appears reasonable. Further similarities include a primary KIE of $\approx 1.35$ at low pH that decreases to a low, constant value at high pH reflecting an apparent p$K$ 8.2–8.4 [48].

The present conclusions are fully compatible with the absence of functional groups essential to acid/base catalysis at the active center of pk- and RgDAAO [13,17–20]. Ser335-OH may play an ancillary role in the transfer of the $H^+$ liberated from the substrate α-$NH_3^+$ to solvent during hydride transfer (Scheme 2). The p$K_a$ determined from kinetic studies, even though it might contain kinetic components, is attributed largely to the microscopic p$K_a$ of the substrate α-amino group. The multiple KIEs strongly support a concerted mechanism for proton transfer and substrate dehydrogenation at low pH and are consistent with the absence of intermediates of any kind, in partial contrast to the results of Denu & Fitzpatrick with pkDAAO [36]. The bulk of evidence therefore unambiguously upholds hydride transfer as the mechanism of flavin-mediated dehydrogenation of amino acids by DAAO.

## ACKNOWLEDGMENT

We thank Prof. M. Pilone for her interest and many fruitful discussions.

## REFERENCES

1. Curti, B., Ronchi, S. & Pilone Simonetta, M. (1992) D- and L-amino acid oxidases. In *Chemistry and Biochemistry of Flavoenzymes* (Muller, F., ed.), pp. 69–94. CRC Press, Boca Raton.
2. Warburg, O. & Christian, W. (1938) Isolierung der prostethischen Gruppe der D-Aminosäure Oxydase. *Biochem. Z.* **298**, 150–155.
3. Schell, M.J., Molliver, M.E. & Snyder, S.H. (1995) D-Serine, an endogenous synaptic modulator: localization to astrocytes and glutamate-stimulated release. *Proc. Natl Acad. Sci. USA* **92**, 3948–3952.
4. Casalin, P., Pollegioni, L., Curti, B. & Pilone Simonetta, M. (1991) A study on apoprotein from *Rhodotorula gracilis* D-amino acid oxidase. *Eur. J. Biochem.* **197**, 513–517.
5. Pilone, M.S., Pollegioni, L. & Butò, S. (1992) Stability and kinetic properties of immobilized *Rhodotorula gracilis* D-amino acid oxidase. *Biotechnol. Appl. Biochem.* **16**, 252–262.
6. Faotto, L., Pollegioni, L., Ceciliani, F., Ronchi, S. & Pilone, M.S. (1995) The primary structure of D-amino acid oxidase from *Rhodotorula gracilis*. *Biotechnol. Lett.* **17**, 193–198.
7. Walsh, C.T., Schonbrunn, A. & Abeles, R. (1971) Studies on the mechanism of action of D-amino acid oxidase. Evidence for removal of substrate α-hydrogen as a proton. *J. Biol. Chem.* **248**, 6855–6866.
8. Rios, A. & Richard, J.P. (1997) Biological enolates: generation and stability of the enolate of N-protonated glycine methyl ester in water. *J. Am. Chem. Soc.* **119**, 8375–8376.
9. Gilbert, H.F., Lennox, B.J., Mossman, C.D. & Carle, W.C. (1981) The relation of acyl transfer to the overall reaction of thiolase I from porcine heart. *J. Biol. Chem.* **256**, 7371–7377.
10. Rudik, I., Ghisla, S. & Thorpe, C. (1998) Protonic equilibria in the reductive half-reaction of the medium-chain acyl-CoA dehydrogenase. *Biochemistry* **37**, 8437–8445.
11. Vock, P., Engst, S., Eder, M. & Ghisla, S. (1998) Substrate activation by acyl-CoA dehydrogenases: transition-state stabilization and p*K*'s of involved functional groups. *Biochemistry* **37**, 1848–1860.
12. Miura, R. & Miyake, Y. (1988) The reaction mechanism of D-amino acid oxidase: concerted or not concerted? *Bioorg. Chem.* **16**, 97–110.
13. Mattevi, A., Vanoni, M.A., Todone, F., Rizzi, M., Teplyakov, A., Coda, A., Bolognesi, M. & Curti, B. (1996) Crystal structure of D-amino acid oxidase: a case of active site mirror-image convergent evolution with flavocytochrome $b_2$. *Proc. Natl Acad. Sci. USA* **93**, 7496–7501.
14. Pollegioni, L., Blodig, W. & Ghisla, S. (1997) On the mechanism of D-amino acid oxidase. Structure/linear free energy correlations and deuterium kinetic isotope effects using *p*-substituted phenylglycines. *J. Biol. Chem.* **272**, 4924–4934.
15. Umhau, S., Pollegioni, L., Molla, G., Diederichs, K., Welte, W., Pilone, M.S. & Ghisla, S. (2000) The X-ray structure of D-amino acid oxidase at 1.2 Å resolution identifies the chemical mechanism of flavin dependent substrate dehydrogenation. *Proc. Natl Acad. Sci. USA* **97**, 12463–12468.
16. Denu, J.M. & Fitzpatrick, P.F. (1992) pH and kinetic isotope effects on the reductive half-reaction of D-amino acid oxidase. *Biochemistry* **31**, 8207–8215.
17. Mizutani, H., Miyahara, I., Hirotsu, K., Nishina, Y., Shiga, K.,

Setoyama, C. & Miura, R. (1996) Three-dimensional structure of porcine kidney D-amino acid oxidase at 3 Å resolution. *J. Biochem. (Tokyo)* **120**, 14–17.
18. Pollegioni, L., Fukui, K. & Massey, V. (1994) Studies on the kinetic mechanism of pig kidney D-amino acid oxidase by site directed mutagenesis of tyrosine 224 and tyrosine 228. *J. Biol. Chem.* **269**, 31666–31673.
19. Harris, C.M., Molla, G., Pilone, M.S. & Pollegioni, L. (1999) Studies on the reaction mechanism of *Rhodotorula gracilis* D-amino acid oxidase: role of the highly conserved Y223 on substrate binding and catalysis. *J. Biol. Chem.* **274**, 36233–36240.
20. Molla, G., Porrini, D., Job, V., Motteran, L., Vegezzi, C., Campaner, S., Pilone, M.S. & Pollegioni, L. (2000) Role of Arginine 285 at the active site of *Rhodotorula gracilis* D-amino acid oxidase: a site-directed mutagenesis study. *J. Biol. Chem.* **275**, 24715–24721.
21. Pollegioni, L., Langkau, B., Tischer, W., Ghisla, S. & Pilone, M.S. (1993) Kinetic mechanism of D-amino acid oxidases from *Rhodotorula gracilis* and *Trigonopsis variabilis*. *J. Biol. Chem.* **268**, 13850–13857.
22. Molla, G., Vegezzi, C., Pilone, M.S. & Pollegioni, L. (1998) Overexpression in *Escherichia coli* of a recombinant chimeric *Rhodotorula gracilis* D-amino acid oxidase. *Prot. Express. Purif.* **14**, 289–294.
23. Strickland, S., Palmer, G. & Massey, V. (1975) Determination of dissociation constants and specific rate constants of enzyme-substrate (or protein–ligand) interactions from rapid reaction kinetic data. *J. Biol. Chem.* **250**, 4048–4052.
24. Gibson, Q.H., Swoboda, B.E.P. & Massey, V. (1964) Kinetics and mechanism of action of glucose oxidase. *J. Biol. Chem.* **259**, 3927–3934.
25. Lumry, R., Smith, E.L. & Glatz, R.R. (1951) Kinetics of carboxypeptidase action. Effect of various extrinsic factors on kinetic parameters. *J. Am. Chem. Soc.* **73**, 4330–4340.
26. Dixon, M. (1953) The effect of pH on the affinities of enzymes for substrates and inhibitors. *Biochem. J.* **55**, 161–170.
27. Cleland, W.W. (1977) Determining the chemical mechanisms of enzyme-catalyzed reactions by kinetic studies. *Adv. Enzymol. Relat. Areas Mol. Biol.* **45**, 273–387.
28. Cleland, W.W. (1982) The use of pH Studies to determine chemical mechanisms of enzyme-catalyzed reactions. *Methods Enzymol.* **87**, 390–405.
29. Fersht, S. (1985) *Enzyme Structure and Mechanism*, pp. 134–154. W.H. Freeman, New York, USA.
30. Porter, D.J.T., Voet, J.G. & Bright, H.J. (1977) Mechanistic features of the D-amino acid oxidase reaction studied by double stopped flow spectrophotometry. *J. Biol. Chem.* **252**, 4464–4473.
31. Fisher, H.F. & Saha, S.K. (1996) Interpretation of transient-state kinetic isotope effects. *Biochemistry* **35**, 83–88.
32. Porter, D.J.T. & Bright, H.J. (1980) Interpretation of the pH dependence of flavin reduction in the L-amino acid oxidase reaction. *J. Biol. Chem.* **255**, 2969–2975.
33. Bunton, C.A. & Shiner, V.J. (1961) Isotope effects in deuterium oxide solution. I. Acid-base equilibria. *J. Am. Chem. Soc.* **83**, 42–47.
34. Schowen, K.B. & Schowen, R.L. (1982) Solvent isotope effects of enzyme systems. *Methods Enzymol.* **87**, 551–606.
35. Pollegioni, L., Falbo, A. & Pilone, M.S. (1992) Specificity and kinetics of *Rhodotorula gracilis* D-amino acid oxidase. *Biochim. Biophys. Acta* **1120**, 11–16.
36. Denu, J.M. & Fitzpatrick, P.F. (1994) Intrinsic primary, secondary, and solvent kinetic isotope effects on the reductive half-reaction of D-amino acid oxidase: evidence against a concerted mechanism. *Biochemistry* **33**, 4001–4007.
37. Ramon, F., Castillon, M.P., de la Mata, I. & Acebal, C. (1998) Chemical mechanism of D-amino acid oxidase from *Rhodotorula gracilis*: pH dependence of kinetic parameters. *Biochem. J.* **330**, 311–314.
38. Fitzpatrick, P.F. & Massey, V. (1982) Proton release during the reductive half-reaction of D-amino acid oxidase. *J. Biol. Chem.* **257**, 9958–9962.
39. Yorita, K., Misaki, H., Palfey, B.A. & Massey, V. (2000) On the interpretation of quantitative structure–function activity relationship data for lactate oxidase. *Proc. Natl Acad. Sci. USA* **97**, 2480–2485.
40. Peterson, K.L., Galitz, D.S. & Srivastava, D.K. (1998) Influence of excision of a methylene group from Glu-376 (Glu376→Asp mutation) in the medium chain acyl-CoA dehydrogenase-catalyzed reaction. *Biochemistry* **37**, 1697–1705.
41. Westheimer, F.H. (1961) The magnitude of the primary kinetic isotope effect for compounds of hydrogen and deuterium. *Chem. Rev.* **61**, 265–273.
42. Hermes, J.D., Roeske, C.A., O'Leary, M.H. & Cleland, W.W. (1982) Use of multiple isotope effects to determine enzyme mechanisms and intrinsic isotope effects. Malic enzyme and glucose-6-phosphate dehydrogenase. *Biochemistry* **21**, 5106–5114.
43. Belasco, J.G., Albery, W.J. & Knowles, J.R. (1983) Double isotope fractionation: test for concertedness and for transition-state dominance. *J. Am. Chem. Soc.* **105**, 2475–2477.
44. Hermes, J.D., Tipton, P.A., Fisher, M.A., O'Leary, M.H., Morrison, J.F. & Cleland, W.W. (1984) Mechanisms of enzymatic and acid-catalyzed decarboxylations of prephenate. *Biochemistry* **23**, 6263–6275.
45. Julin, D.A. & Kirsch, J.F. (1989) Kinetic isotope effect studies on aspartate aminotransferase: evidence for a concerted 1,3-prototropic shift mechanism for the cytoplasmic isozyme and L-aspartate and dichotomy in mechanism. *Biochemistry* **28**, 3825–3833.
46. Schopfer, L.M., Massey, V., Ghisla, S. & Thorpe, C. (1988) Oxidation–reduction of general acyl-CoA dehydrogenase by the butyryl-CoA/crotonyl-CoA couple. A new investigation of the rapid reaction kinetics. *Biochemistry* **27**, 6599–6611.
47. Pawelek, P., Cheah, J.R.C., Macheroux, P., Ghisla, S. & Vrielink, A. (2000) The structure of L-amino acid oxidase reveals the substrate trajectory into an enantiomerically conserved active site. *EMBO J.* **19**, 4204–4215.
48. Grimshaw, C.E., Cook, P.F. & Cleland, W.W. (1981) Use of isotope effects and pH studies to determine the chemical mechanism of *Bacillus subtilis* L-alanine dehydrogenase. *Biochemistry* **20**, 5655–5661.
49. Pollegioni, L., Harris, C., Molla, G., Pilone, M.S. & Ghisla, S. (2001) *FEBS Lett*., in press.